Doctoral Dissertation

Fundamental Study on Highly-Filled Wood-Plastic Composite

Rashmi Kumari

Graduate School of Agriculture
Kinki University
Department of Advanced Bioscience
(Major: Biomaterials)

（英文題目）

Fundamental Study on Highly-Filled Wood-Plastic Composite

Rashmi Kumari

March, 2008

Graduate School of Agriculture
Kinki University
Department of Advanced Bioscience
(Major: Biomaterials)
(Advisor: Prof. Okamoto Tadashi)

（和文題目）

高充填木質プラスチック複合体の基礎研究

近畿大学大学院 農学研究科

バイオサエンス専攻

ラシュミ　クマリ

(指導：岡本　忠)

Submitted to the Graduate School, Kinki University, to fulfill the requirements for the Doctorate Degree.

ABBREVIATIONS

WPC	Wood plastic composite
PLA	Poly (lactic acid)
PLLA	Poly (L-lactic acid)
PP	Polypropylene
MAPP	Polypropylene modified with maleic anhydride
CL	ε-caprolactone
BL	γ-butyrolactone
HA	Hydroxypivalic acid
MALDI-TOF MS	Matrix assisted laser desorption/ionization time-of-flight mass spectrometry
GPC	Gel permeation chromatography
^{1}H NMR	Proton nuclear magnetic resonance
M	Middle lamella
P	Primary wall
S_1	Outer layer of secondary wall
S_2	Middle layer of secondary wall
S_3	Inner layer of the secondary wall
W	Warty layer
MOR	Modulus of rigidity
MOE	Modulus of elasticity
MA	Maleic anhydride
PCL	Polycaprolactone
PCL-g-AA	Acrylic acid grafted polycaprolactone

MFR	Melt flow rate
MFI	Melt flow index
Method A	Compression molding with an oil hydraulic press
Method B	Compression molding with a hot press
AC	Cutter mill compound molded by method A
AH	Hammer mill compound molded by method A
BC	Cutter mill sample molded by method B
EL	Lengthwise extrusion molding composites
EW	Widthwise extrusion molding composites
IX	Injection molding composites without lubricant
IO	Injection molding composites with lubricant
P	Applied load, kgf
L	Distance between support span, cm
B	Composite width, cm
h	Composite thickness, cm
Δy	Elongation or deflection of composite, cm
Wt	Weight gain
Th	Thickness swell
W_1	Weight of the composite containing water
W_0	Weight of the dried composite
t_1	Thickness of wet composite
t_0	Thickness of dry composite
SD	Standard deviation
T_g	Glass transition temperature

DMTA	Dynamic mechanical thermal analysis
E'	Storage modulus
E''	Loss modulus
CTE	Coefficient of thermal expansion
Tan δ	Dissipation factor or loss tangent, E'/E''
ΔL	Change in length (mm)
ΔT	Change in temperature (°C)
L_0	Initial composite length (mm)
b.p.	Boiling point
m.p.	Melting point
DSC	Differential scanning calorimetry
T_c	Crystallization temperature
T_m	Melting temperature
WF	Wood fiber
BF	Bamboo fiber

CONTENTS

CHAPTER 1

Introduction and Background

1.1 Wood plastic composite (WPC): Applications and research issue

Interests in wood fiber-reinforced polymer composites, or bio-based composites, have grown tremendously because of their low material costs, light weight, high specific modulus (modulus over density), and environment friendly appeal [1]. To convert low-value wood resources into high-value products, researchers are combining wood fiber with thermoplastic resin, resulting in wood plastic composites. Thermoplastic resins, such as polypropylene, polyethylene, polystyrene, and polyvinyl chloride, soften when heated and harden when cooled. This property allows wood to be mixed with the plastic to form a composite product. Additives are also often used in WPCs. Additives are materials that are added in small amounts to enhance properties. For example, lubricants improve surface appearance and processing; coupling agents improve adhesion between the wood and plastic components. Other possible additives include colorants, light stabilizers, foaming agents, and thermoplastics. The resulting WPCs can be easily processed into various shapes by three common molding methods for WPCs are extrusion, injection, and compression molding. Several factors influence processing WPCs such as moisture can disrupt many thermoplastic processes, resulting in poor surface quality and voids. Mechanical and physical properties, such as strength, stiff-ness, impact resistance, density, and color, are important considerations in many WPCs applications. For example, automotive applications take advantage of a lower specific gravity, household products, such as paintbrush handles, scissor handles, and flowerpots, take advantage of the aesthetics, resulting in a product that can look like wood but can be processed like a plastic. Semi-structural building applications, such as decking, roof tiles, and window trim, also take advantage of the wood look and offer improved thermal and creep performance compared with unfilled plastics. WPCs are currently used in railing systems (deck boards, stairs, posts and post rails, handrails and

bottom rails, post caps, balusters, and other small accessories)[2]. Construction, transportation, industrial, and consumer applications for wood plastic composites are all on the rise. WPC have been primarily produced with a low and medium percentage of wood/cellulose. Products typically contain approximately 50% (by weight) wood/cellulose, although some composites contain very little wood/cellulose and others as much as 60% [3-7]. Wood/cellulose content may range from 70% to 90% and the interfacial adhesion between wood/cellulose particles and polymers can be improved by adding a compatibilizer. One of the major challenges for WPC is to optimize the content of the wood/cellulose in WPCs to reduce costs and compete with solid wood and engineered wood/cellulose composite products. However, extruded wood-plastic composites are a relatively new product whose market growth has been rapid. The engineering design of extrusion operations requires proper knowledge of the flow mechanism of these highly filled melts. The formulating of wood plastic formulations also requires reliable evaluation of flow performance of the composite melts. Rheological characterization affords knowledge about both the fundamental flow behavior of the highly filled plastics and practical methods for evaluating the flow performance for process development. The technical challenges are to overcome flow problems, the low bulk density of the wood as well as separation problems of the composite mixture. Therefore, advancing this area of knowledge for this new material class is important for further developments of the science and industry [4, 8, 9].

Recently, interest has been growing in developing biomass-based plastics to reduce greenhouse gas (CO2) emissions and to conserve petroleum resources. Biomass-based plastics include microbial products such as polyhydroxybutylate, chemosynthesis products such as poly (lactic acid) (PLA), and chemically modified natural products such as esterified starch and cellulose acetate. Petroleum-based polymers (such as polypropylene, polyethylene etc.) of WPCs can be replaced by bio plastic and resulting matrix will create a complete bio based plastic. Poly (L-lactic acid) (PLLA) shows a valuable alternative to petroleum-based polymers for uses as plastics, fibers, and

coatings. Brittleness, water resistance and cost limit the applications of wood/PLLA composites.

This work is divided in two different parts. The first part reports the effects of materials on processibility and performance of cellulose micro fibers, random polypropylene (PP), and the coupling agent polypropylene modified with maleic anhydride (MAPP). Composites prepared with different fiber lengths (120, 300, and 900μm) of cellulose and with the different content (70, 80 and 90%) were studied. A study on the mechanical and water absorption of compression, extrusion, and injection molding composites is presented here. Melt flow characteristics such as melt index, have been studied with special reference to the effect of blend ratio, cellulose fiber length, temperature, and die diameter. The effect of the different fiber length and content of cellulose on the morphology and water absorption of the composites is discussed.

The second part consists of the study of WPC with an 80/20 wood fiber/poly (L-lactic acid) composition containing modified PLLA as a compatibilizer. For modification of PLLA, PLLA were copolymerized by ε-caprolactone (CL), γ-butyrolactone (BL), and hydroxypivalic acid (HA). The resulting copolymers were characterized by various analytical techniques including matrix assisted laser desorption/ionization time-of-flight mass spectrometry (MALDI-TOF MS), gel permeation chromatography (GPC), and proton nuclear magnetic resonance spectra (^{1}H NMR). To improve compatibility and mechanical properties of wood/ PLLA or bamboo/PLLA, poly (lactic acid-co-caprolactone) (P (LA-co-CL)) copolymer produced in this study.

1.2 Wood fiber: Structure and composition

Wood is a heterogeneous, hygroscopic, cellular and anisotropic material. It is composed of fibers of cellulose (40%–50%) and hemicellulose (15%–25%) held together by lignin (15%–30%) [10]. Wood fibres, are a structural cell element of wood that are extracted

from trees, straw, bamboo, and other sources. Wood fibre is primarily extracted from hardwood (dicotyledonous) trees and softwood (coniferous) trees. It is made commercially by chipping and grinding.

1.2.1 Structure of wood

The primary structural building block of wood is the fiber cell. The fiber cell wall is build up by several layers, namely (Figure 1.1) middle lamella (M), primary wall (P), outer layer of secondary wall (S_1) middle layer of secondary wall (S_2), inner layer of the secondary wall (S_3) and warty layer (W) [11]. Each layer is composed of a combination of three chemical polymers: cellulose, hemicellulose, and lignin. The cellulose and hemicellulose are linear polysaccharides (i.e., hydrophilic multiple-sugars), and the lignin is an amorphous phenolic (i.e., a three dimensional hydrophobic adhesive). Cellulose forms long unbranched chains and hemicellulose forms short branched chains. Lignin encrusts and stiffens these polymers.

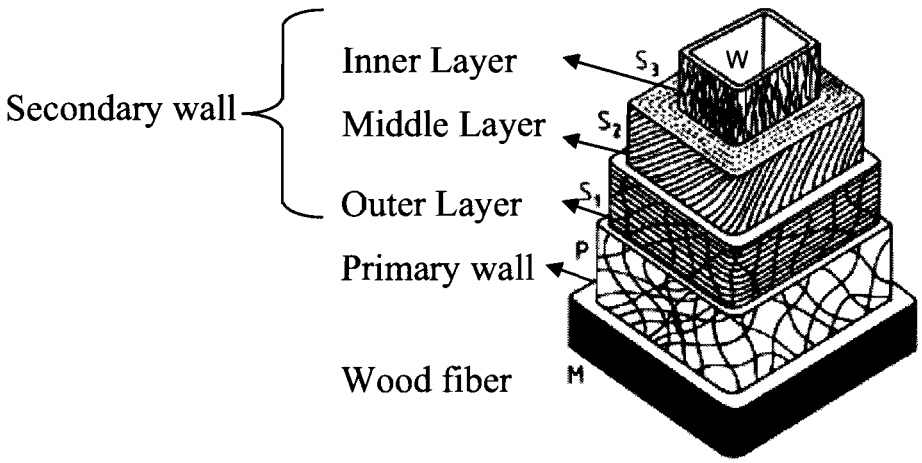

Figure 1.1. The structure of wood fibers

1.2.2 Cellulose

Cellulose is a biopolymer that wood use as the primary building block for their cell walls and has economic significance because it is 40% to50% constituent of wood.

Cellulose is a high-molecular-weight (10^6 or more) linear polymer of β-(1 → 4)-D-glucopyranose units in the $^4C_1$ conformation (Figure 1.2). The fully equatorial conformation of β-linked glucopyranose residues stabilizes the chair structure, minimizing flexibility. Glucose anhydride, which is formed via the removal of water from glucose, is polymerized into long cellulose chains that contain 5000-10000 glucose units. The basic repeating unit of the cellulose polymer consists of two glucose anhydride units, called a cellobiose unit [12]. The intermolecular bonds and intramolecular hydrogen bonds determine the internal structure and control the mechanical properties of cellulose as well as the behavior of cellulosic materials as a result of a moisture change. When moisture is brought into contact with cellulose, water molecules diffuse into non-crystalline domains, swell the structure and form new hydrogen bonds. Furthermore, they may create water bridges instead of the hydrogen bonds present in dry cellulose. Intermolecular bonds are most easily affected in this way. In contrast, the crystalline regions in cellulose are almost inaccessible to moisture [13].

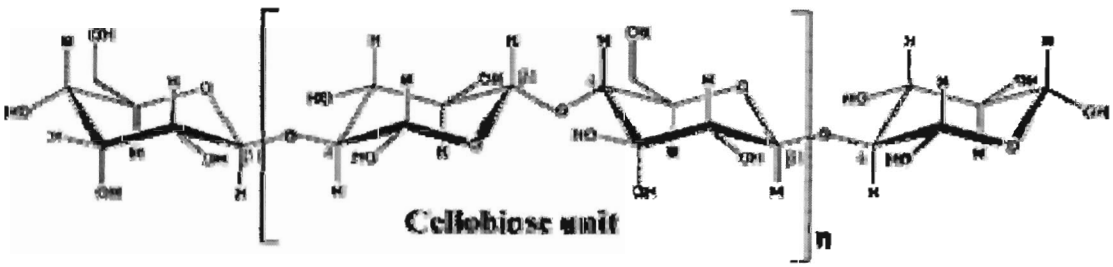

Figure 1.2. Structure of cellulose

1.2.3 Hemicelluloses

In general, the hemicellulose (20–40%) fraction of woods consists of a collection of polysaccharide polymers with a lower DP than cellulose (average DP of 100–200) and containing mainly the sugars D-xylopyranose, D-glucopyranose, D-galactopyranose, L-arabinofuranose, D-mannopyranose, D-glucopyranosyluronic acid, and D-galactopyranosyluronic acid with minor amounts of other sugars. Hemicelluloses usually consist of more than one type of sugar unit and are sometimes referred to by the

sugars they contain, for example, galactoglucomanan, arabinoglucuronoxylan, arabinogalactan, glucuronoxylan, glucomannan, etc. [14]. Hardwood hemicelluloses contain mostly xylans, whereas softwood hemicelluloses contain mostly glucomannans [15]. The galactoglucomannan is the principal hemicellulose (approximately 20%), with a linear or possibly slightly branched chain with β-(1→4) linkages. A representative structural formula for softwood galactoglucomannan is represented in Figure 1.3.

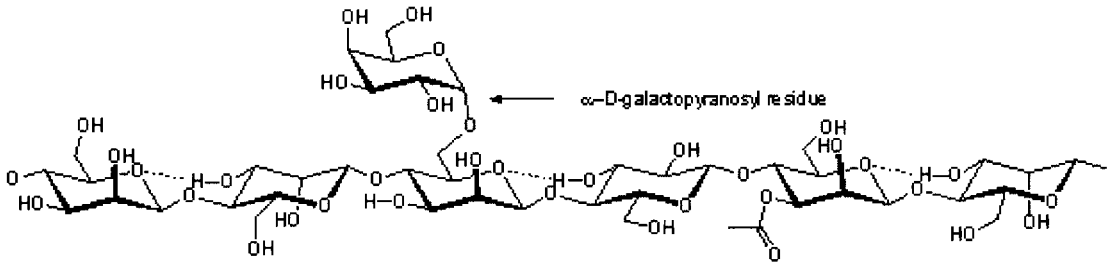

Figure 1.3. Structure of softwood galactoglucomannan

1.2.4 Lignin

Lignin is a necessary constituent in the cell walls of all vascular plants. It is one of the most abundant biopolymers, and a considerable part of the carbon fixed by photosynthesis is consumed by lignin biosynthesis. The biological functions of the polymer are as follows: (1) they give stiffness and strength to the secondary wall of vascular plants. The lignified cell wall can be seen as a composite, with cellulose microfibrils giving stiffness to the material. (2) They make the cell wall hydrophobic. This allows the development of tissues for efficient water transport in vascular plants. (3)They are an obstacle to microbial attack. The presence of lignin makes woody tissues compact that molecule as large as proteins cannot penetrate the tissue. Thus, wood is much more resistant to microbial attack than are non-lignified cellulosic materials, such as cotton, and many wood. Lignin is polymerized in the wood from the monolignols sina-pyl, coniferyl, and *p*-coumaryl alcohol. Hardwood lignin (in dicotyledons) originates mainly from sinapyl alcohol and coniferyl alcohol, whereas softwood lignin (in coniferous trees and gingko) is made mainly from coniferyl alcohol. As a

biomacromolecule, lignin is unusual in having a complex network–type structure (Figure. 1.4) [16].

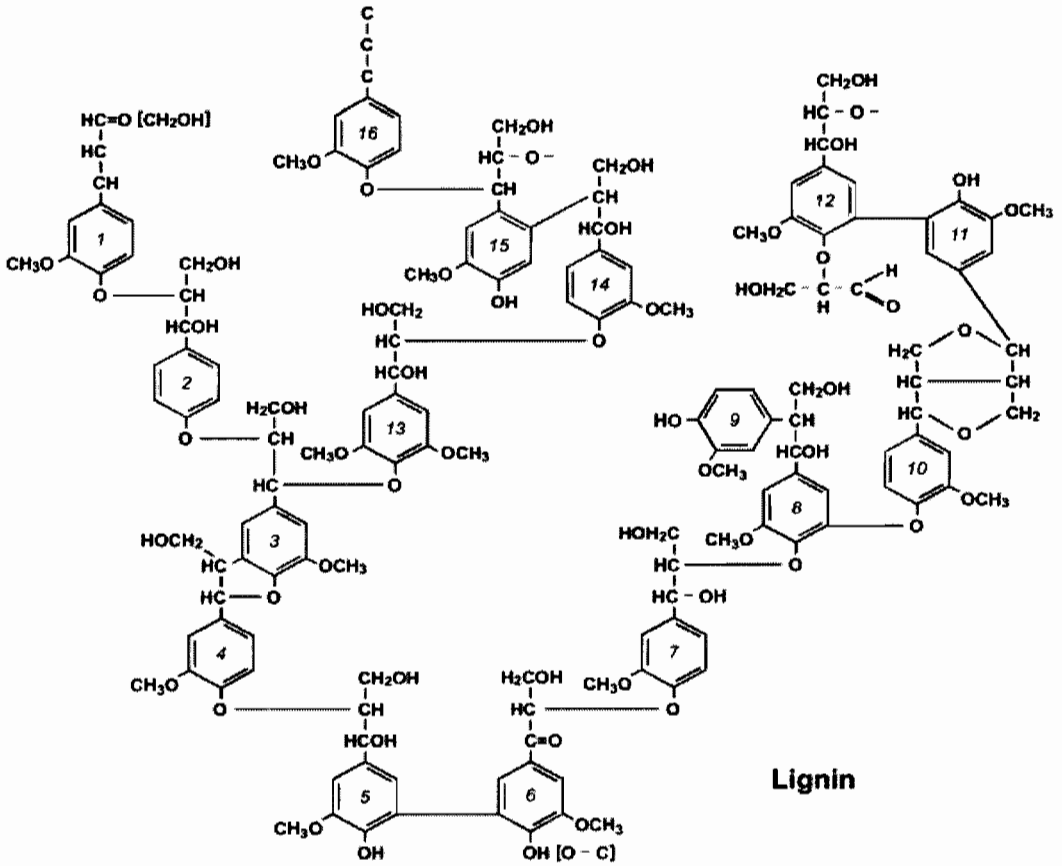

Figure 1.4. Structure of Lignin

1.3 Wood/plastic composites compatibility

1.3.1 Cellulose/polypropylene compatibility and interaction

The combination of synthetic thermoplastic polymers and wood is normally problematic because wood is a hydrophilic, porous, hygroscopic and polar material and synthetic thermoplastics are hydrophobic. The major issue in achieving true reinforcement is the inherent incompatibility between the hydrophilic fibers and the hydrophobic polymers, which results in poor adhesion and, therefore, in poor ability to transfer stress from the matrix to the reinforcing fibers. A number of investigators have explored the ability of

additives to enhance the adhesion and thereby improve the properties such as tensile and flexural strength of these composite materials, the techniques adopted include plasma treatment, graft copolymerization, silane treatment and treatments with other chemicals. MAPP is a widely used coupling agent within polypropylene based composites. The addition of MAPP shows a marked increase in the modulus of rupture (MOR) and modulus of elasticity (MOE) of polypropylene based composites, indicating some form of interaction between the matrix and the MAPP. MAPP exists in two forms, an anhydride and a di-carboxylic acid form. Heinen et al. determined the most probable structure of MAPP (Figure 1.5) using smaller model compounds studied in solution with ^{13}C NMR spectroscopy (Heinen, 1999). This structure contains the anhydride form of MA grafted on the PP backbone. The current hypothesis states that maleic anhydride (MA) functional groups are capable of chemically bonding with wood, via ester bonds or secondary interactions such as hydrogen-bond (Figure 1.5) [17, 18, 30, 31]. The chemical interactions between MAPP and cellulose suggest esterification as the main interaction with a possibility of hydrogen bonding (Figure 1.5). Avella et al. proposed that MA groups migrate towards the fiber surface due to the polar/non-polar interactions, thus increasing the probability of bonding between the MA and the hydroxyl groups on the wood fibers/cellulose [19].

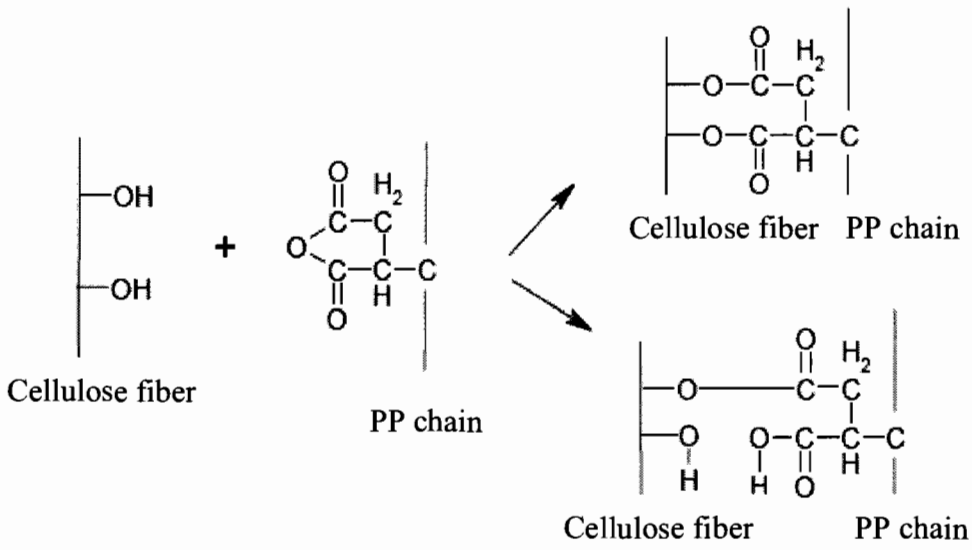

Figure 1.5. Esterification of cellulose

1.3.2 Wood/poly (lactic acid) composites compatibility

The formulation of biodegradable composites is gaining interest because of decreasing fossil resources and environmental regulations. In this way, ''green bio-composites'' or ''eco-composites'', obtained by compounding wood fiber with renewable resource-based poly(lactic acid) polymers, open the way to the next generation of sustainable, environmentally friendly, eco-efficient materials, products, and processes. In spite of its relative weakness and about 60°C melting point that is too low for many applications, polycaprolactone (PCL) has recently received much attention due to its flexibility and biodegradability. Chin-San Wu et al. investigated systematically the properties of PCL/wood flour and acrylic acid grafted PCL (PCL-g-AA)/wood flour blends and found that due to the generation of ester carbonyl functional group from reaction between -OH group of WF and –COOH group of PCL-g-AA copolymer [20]. Lee et al. reported that interfacial properties between bamboo fiber and PLA were improved after the addition of bamboo fiber-esterified maleic anhydride [21].

1.4 Processing

Typical blending of wood with a thermoplastic involves the plastic-filler reinforcement to be shear mixed at temperatures above the softening point of the plastics. The heated mixture is then typically extruded into "small rods" that are then cut into short lengths to produce a conventional pellet (Figure 1.6). The pellets can then be used in typical injection, extrusion or compression molding processes. Processing the wood without loss of fiber properties is a major issue. The processing temperatures used in the plastic industry are usually above the decomposition temperature of the materials. Temperatures, above 180°C, result in decomposition of wood so processing temperatures lower that 180°C, are needed if a wood material is used as a filer. Thermoplastics with a high melt flow index and low softening temperatures are usually used [22].

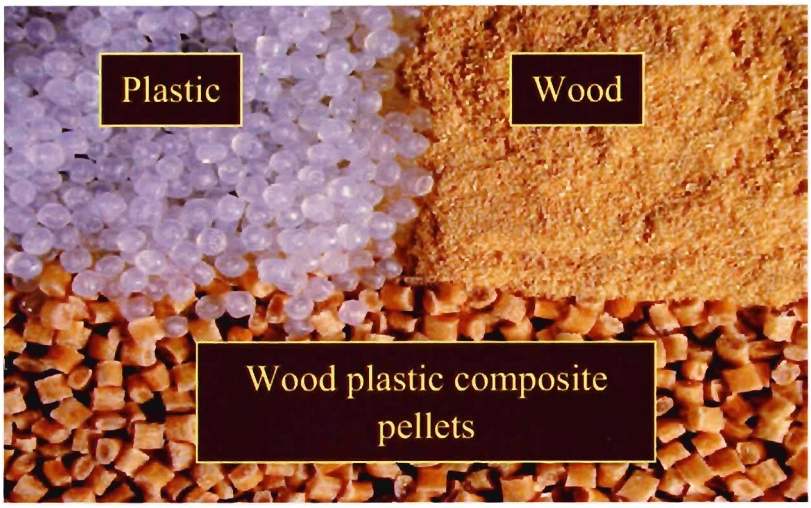

Figure 1.6. Pellets after processing of wood plastic composites

PART 1

EFFECT OF MATERIALS ON PROCESSIBILITY AND PERFORMANCE OF CELLULOSE/PP/MAPP

CHAPTER 2

Processing and Melt Flow Behavior of Cellulose/Polypropylene/MAPP Composites

2.1 Introduction

This chapter presents standard procedures for processing and flow behavior for cellulose/PP/MAPP composites. The first step in producing a WPC is to determine raw materials, and its amounts, which will produce a WPC that meets the processing and performance requirements. Manufacturing melt-blended composites is usually a two-step process consisting of compounding and molding. In the compounding step, wood/cellulose fiber and additives are combined with molten thermoplastic to produce a homogeneous composite material. Generally, melt mixing techniques applied to WPC are twin screw extruder, two-roll mill, turbine mixer, ball mill etc. Three common molding methods for WPCs are extrusion molding, injection molding, and compression molding. Melt flow studies of compounds are very important for optimizing the processing conditions and to design processing equipments like injection molding machines, extruders, and dies required for various products. During the processing, the blend may undergo various changes. Better knowledge of the processing defects will help to introduce the suitable remedies to optimize the processing problems [23].

2.2 Experimental Method

2.2.1 Materials

The materials used in the study of this part were cellulose, a thermoplastic polymer, polypropylene (PP), and a coupling agent MAPP, which is polypropylene modified with maleic anhydride. The thermoplastic polymer was a random PP (PM930V, MFR 30 g/10 min, density 0.9 g/cm^3) supplied by SunAllomer (Tokyo, Japan). Three different length of fibrous cellulose (BE00, BC200, B400) were products of Rettenmaier and

Söhne (Rosenberg, Germany), produced from softwood. The basic properties of all the cellulose powders are listed in Table 2.1. The coupling agent was MAPP (umex1010) obtained from Sanyo Kasei (Tokyo, Japan).

Table 2.1. Basic properties of all cellulose powers

Color	BE00	BC200	B400
	White	White	White
Structure	Short fiber	Medium fiber	Long fiber
Fiber Length (μm)	120	300	900
Fiber diameter (μm)	20	20	20
Bulk density (g/l)	150-180	60-80	20-40

2.2.2 Blending procedure

The cellulose fibers, PP and MAPP were sequentially fed into a conical twin-screw extruder (Model Taitan 80, Cincinnati Co.). The temperature profile of the extruder from cylinder 1 through cylinder 4 was kept between 230°C and 180°C and the extruder was operated at screw speed 7rpm. After the compounding, the composite was then crushed with a cutter mill (wood grinder) or a hammer mill and used for compression molding. Extruded strands were also palletized. Pellets were used for extrusion molding and injection molding composites. Crushed pellets used for injection samples were also prepared with the addition of 2 wt% calcium stearate as a lubricant. The compositions of cellulose powder, PP and MAPP were listed in Table 2.2.

2.2.3 Melt flow index

Melt flow index (MFI), that is, the weight of polymer in grams extruded in 10 min through a capillary, was determined using Dynisco Melt flow indexer LMI 4000 (Figure 2.1) series as Japan Industrial Standards (JIS) K 7210. The applied loads and die

diameters were 5 and 10 kg, and 6 and 7 mm, respectively. The measurement was carried out at 230°C.

Table 2.2. Composition of cellulose powder, PP and MAPP

No.	Composition (wt%)				
	Cellulose			PP	MAPP
	BE00	BC200	B400	PM930V	UMEX1010
1	80			18	2
2		70		28	2
3		80		18	2
4		90		8	2
5			80	18	2

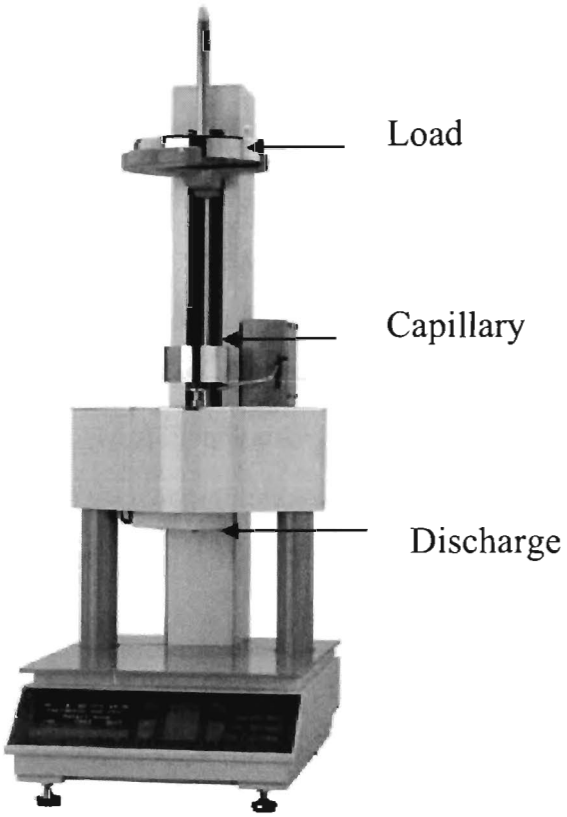

Figure 2.1. Melt flow indexer

2.2.4 Compression molding

The specimens for mechanical tests were prepared by compression molding with an oil hydraulic press HP-1B-P (Method A) at 200°C. Other press conditions were set to bring close to the average of theoretical densities of components, plastic (TD=0.89-0.92) and wood (TD=1.5). The average theoretical density of a wood/cellulose plastic composite made with ratio 80/20 is 1.38. The theoretical density was calculated on the basis of weight percent and the density of components. Specimens for analysis were cut from the sheets of the cutter mill compound molded by method A (AC) and the hammer mill compound molded by method A (AH). The blends were also compression molded using a steel mold (dimensions: 0.25×8×10cm) by a Shinto hot press Model HCC-BSN-2 (Figure 2.2) (Method B) at temperature 220°C, under the pressure of 11MPa for 5min and cooled to room temperature. Teflon films were used to avoid the adhesion of MAPP to the stainless surface of the mold. Three standard specimens (dimensions: 0.25×2.5×10cm) were cut from the sheet of the cutter mill sample molded by method B (BC) as shown in Figure 2.3.

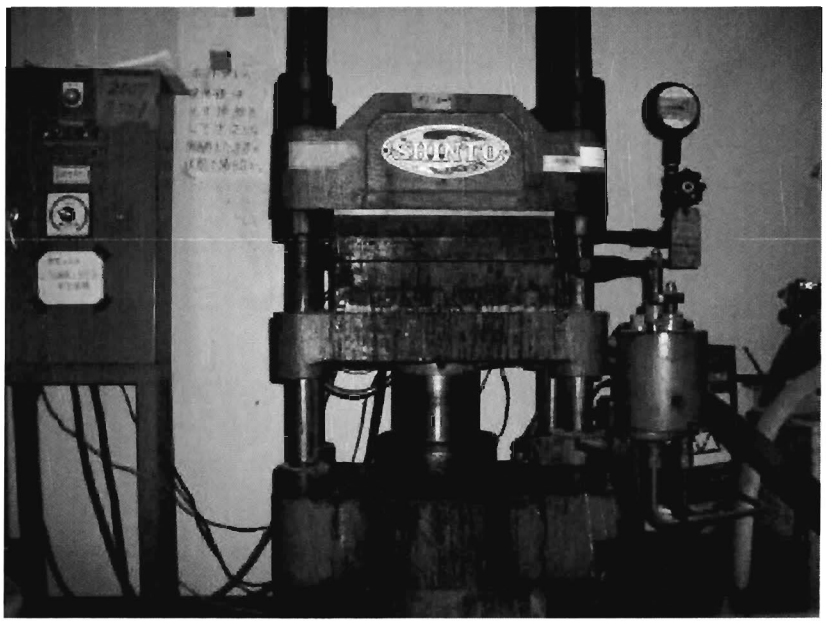

Figure 2.2. Shinto hot press Model HCC-BSN-2

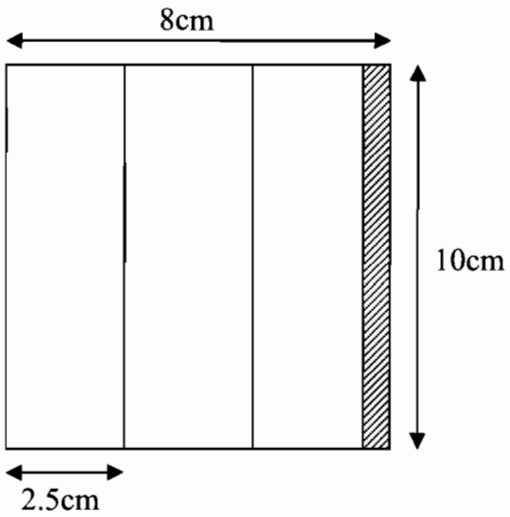

Figure 2.3. Three standard cutting specimens (Dimensions: 0.25×2.5×10cm) from the sheet of the cutter mill sample molded by method B.

2.2.5 Extrusion molding

Pellets were extruded as thick long sheets in this process. Pellets were fed into a conical twin-screw extruder model Titan 68 (Figure 2.4, Taiyo Gosei, Kagawa, Japan). The molding conditions were as follows: temperatures on cylinder 1 to cylinder 4 were held between 215°C and 170°C and the temperature for heating zone to cooling zone of exit die was to be 175°C to 45°C. The extruder was operated at screw speed 5 rpm. The resulting sheets were cut lengthwise (EL) (dimensions: 0.92×2.5×10.8cm) and widthwise (EW) (dimensions: 0.9×1.9×11.9cm) to make the test specimens as shown in Figure 2.5.

Figure 2.4. Conical twin-screw extruder model Titan 68

Figure 2.5. Standard cutting specimens of of extrusion molding composites. *EL,* Lengthwise (Dimensions: 0.92 × 2.5 × 10.8cm); *EW,* Widthwise (Dimensions: 0.9 × 1.9 × 11.9cm)

2.2.6 Injection molding

The injection molder used was a Roboshot a-100C (Fanuc). The molding conditions were listed in Table 2.3. The resulting dumbbell-shaped mold without lubricant (IX)

and mold with lubricant (IO) were molded as shown in Figure 2.6. A regular injection nozzle was used, with a nozzle diameter of 2 mm. The dumbbell-shaped molds were cut into rectangular shape (Dimensions: 0.4×1×8cm) to make the test specimens for mechanical test.

Figure 2.6. Dumbbell-shaped molds from injection molding method

Table 2.3. Molding conditions of injection mold

No.[a]		Lubricant (wt%)	Injection Time (sec)	Nozzle Temp (°C)	Peak Pressure (MPa)
1	IX	0	0.29	210	29.6
	IO	2	0.30	195	29.4
2	IX	0	0.57	185	22.7
	IO	2	0.60	185	23.9
3	IX	0	0.29	210	29.5
	IO	2	0.31	195	29.5

IX, Injection mold without lubricant; *IO*, Injection mold with lubricant; [a] No. of composition same as in Table 2.2.

2.3 Results and discussion

2.3.1 Melt flow index

Flow behavior of compound is one of the most important factors to be considered when establishing injection molding and extrusion molding [4, 8]. Figures 2.5 and 2.6 show the experimental results obtained for the melt flow index of pellets measured at 230°C. The melt flow rate provides valuable information about the flow behavior of materials. It is found that the MFI value decreases with an increase of cellulose content because the incorporation of rigid weight of cellulose to the polymeric matrixes limits their free mobility, increasing the material apparent viscosity. Formulations with 90% cellulose loading did not flow and MFI values were unable to be measured. Caraschi and Leão et al. [24] obtained similar results in which the increase of fiber amount decreased the MFI value. As for the effect of cellulose size, pellets containing 300μm fiber length cellulose showed lower values than pellets containing 120μm cellulose. For each pellet, an increase in die diameter increased the melt flow, especially with 10-kg load. With 5-kg load, the 80% cellulose content compound could not be measured with 6-mm diameter. However, it could be measured with 7-mm die. With 10-kg load, compound with 80% cellulose content could be measured with both die of 6-and 7-mm diameter. The compound with 70% (w/w) cellulose content had remarkably low fluidity relative to a general plastic material. Therefore, it was concluded that desirable conditions for measurement were 5-kg load/7-mm die and 10-kg load/6-mm die. A good extrusion-molded and injection-molded composite could be obtained at this temperature 230°C. However, degradation of cellulose fibers starts at 180°C [25].

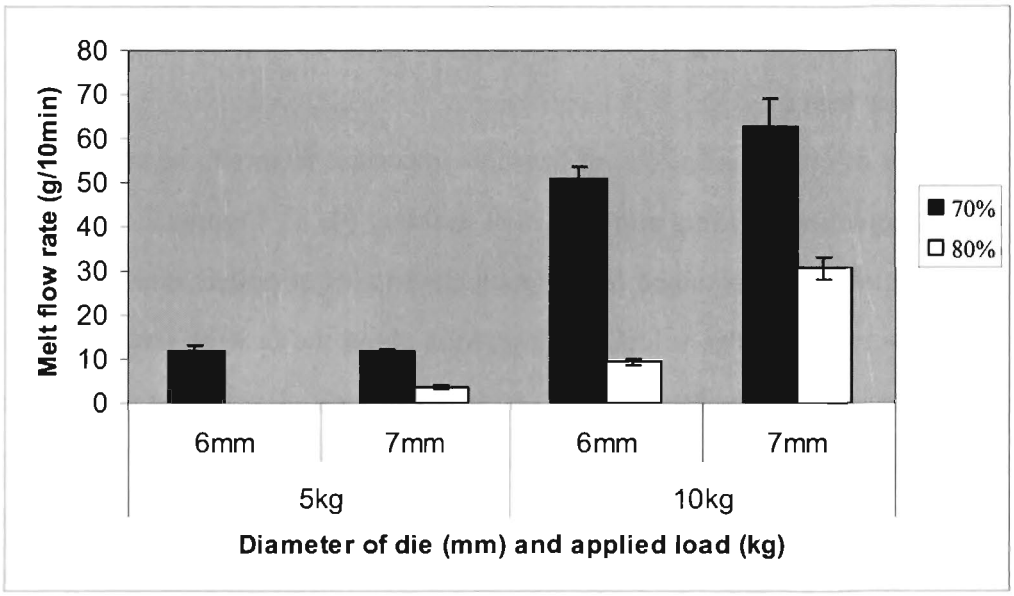

Figure 2.5. Melt flow index of 300μm fiber length cellulose pellets against fiber weight percent. *Filled bars*, Cellulose/PP/MAPP=70/28/2; *open bars*, Cellulose/PP/MAPP=80/18/2

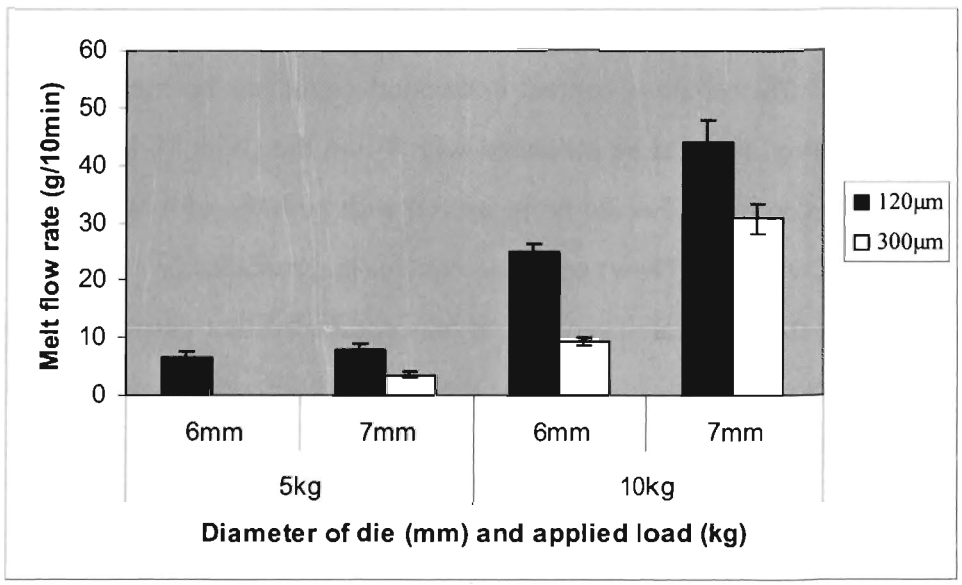

Figure 2.6. Melt flow index of pellets with different fiber lengths of 80 wt% cellulose and 20wt% plastic content. *Filled bars*, Cellulose fiber length=120μm; *open bars*, Cellulose fiber length=300μm

2.3.2 Feasibility of compression, injection, and extrusion molding

Table 2.4 illustrates the feasibility of compression, injection, and extrusion molding. It is noted that the feasibility is highly dependent on both the fiber content and length of fiber as shown in previous section (2.3.1). It has been shown that the feasibility of extrusion molded composites depend significantly with high resin content but not as much by the fiber length. On other hand it has been also found that composites were moldable by injection molding only when both high cellulose fiber content and smaller fiber length were met. As compression molded composites are feasible in all cases it reveals that compression molding is more compatible.

Table 2.4. Feasibility of compression, injection and extrusion molding of compositions of cellulose fiber/PP/MAPP

No.[a]	Molding Process				
	Compression		Extrusion	Injection	
	Hammer	Cutter		IO	IX
1	○	○	○	○	○
2	○	○	×	○	○
3	○	○	○	○	○
4	○	○	×	×	×
5	○	○	×	×	×

IO, Injection mold with lubricant; *IX*, Injection mold without lubricant; ○, indicates molding feasible ; ×, indicates molding not feasible; [a] No. of composition same as in Table 2.2.

2.4 Conclusions

Composites of MAPP, cellulose and polypropylene were produced by compounding in a conical twin-screw extruder. Processibility with high resin content and small fiber length is difficult than its counterparts at low resin loadings and large fiber length. Unfortunately, feasibility studies on extrusion molding and injection molding of the highly loaded wood/cellulose plastics are scarce in the open literature. Two extrusion-molded composites and three injection-molded composites have been developed. The cellulose content dependency of flowability is similar to the prediction, indicating that the deforming capacity of cellulose facilitates the denser packing of the filler particles. The melt flow rate of the composite filled with 90 wt% of cellulose and composite of fiber length 900μm does not show any flowability. These features are not unique for the cellulose fiber and provide a rheological basis for achieving better processibility with low cellulose content and small fiber length than its counterparts at high cellulose loadings and large fiber length.

CHAPTER 3

Mechanical Properties and Water Absorption of Cellulose/Polypropylene/MAPP Composites

3.1 Introduction

A study on the mechanical and water absorption properties of compression, extrusion and injection molded composites will be presented here. Reviews of WPCs have shown that they have good potential to improve the water resistance of woody composites, because thermoplastic polymers are highly hydrophobic [6, 43]. Some researchers believe that if the interaction can be improved, the composites could be given better mechanical properties and better particle dispersion [44]. It is known that the mechanical and physical properties of WPC products are affected by a number of factors, such as the volume fraction and aspect ratio of fiber, dispersion level, fiber orientation, fiber–polymer adhesion, which are dependent on the mixing time and processing temperature. The most important factor on the mechanical properties of the composites is the fiber–matrix adhesion. The incompatibility between polar cellulose fibers and hydrophobic polymers results in inferior mechanical properties due to poor interfacial bonds. Current concepts of the methods applied to improve the fiber–matrix interfacial adhesion include molecular chain entanglements, good mechanical contact, the matching of surface tensions, and the formation of chemical and physical bonds through the use of chemical coupling agents [26]. The one most common method used to determine the mechanical properties of WPCs is the three-point bending test. At present, the three-point bending test is the only test method for determining modulus of rupture (MOR) and modulus of elasticity (MOE) of composites. In three-point bending test, the MOR and MOE are determined with the use of following equations, respectively

$$\text{MOR} = \frac{3PL}{2bh^2} \text{ (kgf/cm}^2\text{)}$$

$$\text{MOE} = \frac{\Delta PL^3}{4\Delta ybh^3} \text{ (kgf/cm}^2\text{)}$$

Where:

P=Applied load, kgf

L=Distance between support span, cm

b=Composite width, cm

h=Composite thickness, cm

Δy= elongation or deflection of composite, cm

3.2 Experimental Method

3.2.1 Mechanical test

The small rectangular specimens were tested on a Shinto Model TCM-500 and the load-deformation curve was determined. The support span depended on the length of the mold and the crosshead speed was 5.0 mm/min. At least 12 specimens were tested for each composite in accordance with JIS A5908. All specimens showed a yielding fracture mode. The modulus of rupture (MOR) and modulus of elasticity (MOE) were calculated from the load–deformation curve. The MOR was defined as the first point on the load– deformation curve to show a slope of zero. The MOE was determined from the slope in the initial elastic region of the load–deformation curve.

3.2.2 Water absorption test

The samples based on increasing fiber length of cellulose and cellulose content of compression molding were tested for water absorption for from 0 to 24 hour under atmospheric pressure at room temperature. Water absorption in weight gain (Wt), and thickness swell (Th) was calculated by the equation (1) and equation (2), respectively:

$$Wt = (W_1 - W_0)/ W_0 \quad (1)$$

$$Th = (t_1 - t_0)/ t_0 \quad (2)$$

Where, W_1, W_0, t_1, and t_0 are the weight of the composite containing water, weight of dry composite, thickness of wet composite and thickness of dry composite, respectively.

3.3 Results and Discussion

3.3.1 Mechanical test

Compression molding

Method A: The effects of PP content on modulus of rupture (MOR) and modulus of elasticity (MOE) of the cellulose /PP/MAPP composites are shown in Figures 3.1 and 3.2, respectively. The compound crushed by a hammer mill (AH) tends to decrease the MOR with the increase of resin content from 20 to 30 wt%. If the extent of phase separation has been very severe, the strength of the materials will decrease [44]. The MOR of cutter mill composite (AC) simultaneously increased with an increase in PP content, suggesting that a relatively strong interaction exists between cellulose and PP [44]. The cutter mill compound contains fibers of a high average aspect ratio, and so they orient easily under conditions of high fluidity. Since the press pressure of method A is high, it is easy for a cutter mill compound to orient under high fluidity press conditions of 70 wt% cellulose content. The bending strength and the elastic modulus were high as expected. Since a compound of 80 wt% cellulose content had low fluidity, the resulting composite did not differ much from the composite of hammer mill compound. By the way, MOE of the composite AC was decreased as increases fiber length of cellulose.

Method B: There is a tendency of the bending strength and the elastic modulus decreasing with the resin content. However, the tendency is not remarkable like the composite AH.

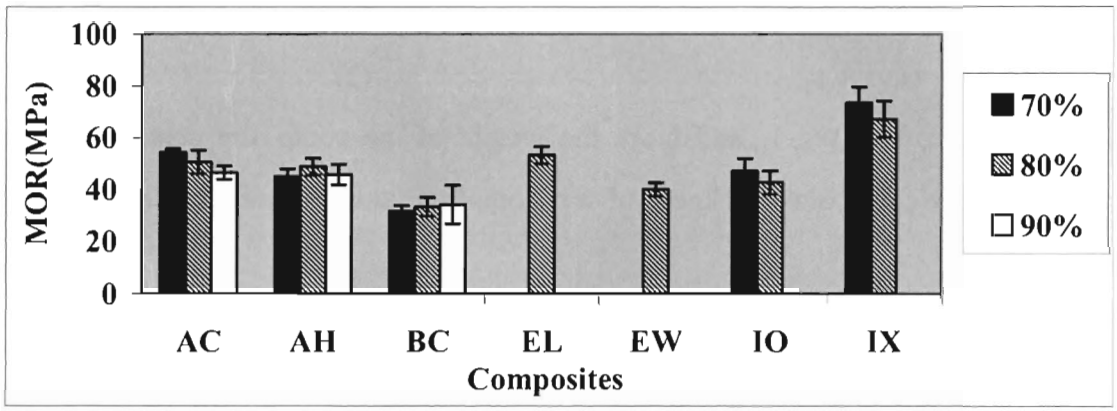

Figure 3.1. Effects of fiber content on MOR of composites with 300μm cellulose; Error bars represent standard deviation. *Filled bars*, Cellulose/PP/MAPP=70/28/2; *shaded bars*, Cellulose/PP/MAPP=80/18/2; *open bars*, Cellulose/PP/MAPP=90/8/2

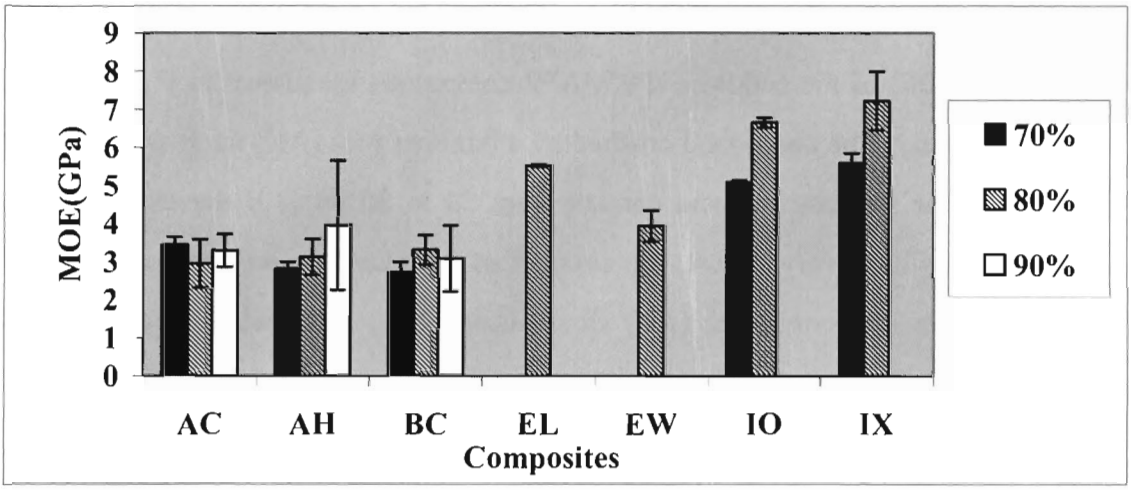

Figure 3.2. Effects of fiber content on MOE of composites with 300μm cellulose; Error bars represent standard deviation. *Filled bars*, Cellulose/PP/MAPP=70/28/2; *shaded bars*, Cellulose/PP/MAPP=80/18/2; *open bars*, Cellulose/PP/MAPP=90/8/2

Effect of fiber length of cellulose

In Figures 3.3 and 3.4, the enhancing effect of the fiber length of cellulose in the mechanical properties is clearly shown. The progressive increases in MOR of the composites AH, EW, EL, IO, and IX, as the fiber length of cellulose was increased. While, 300 and 900 μm fiber length mold have not much effect on MOE. In contrast, MOE of the composite BC increased as increases the fiber length. However, mechanical

properties of 900μm fiber length composite showed high standard deviation (SD). Since a fiber is long, resin did not disperse uniformly. It is also suggesting that there is lack of a certain degree of miscibility between long cellulose and PP/MAPP.

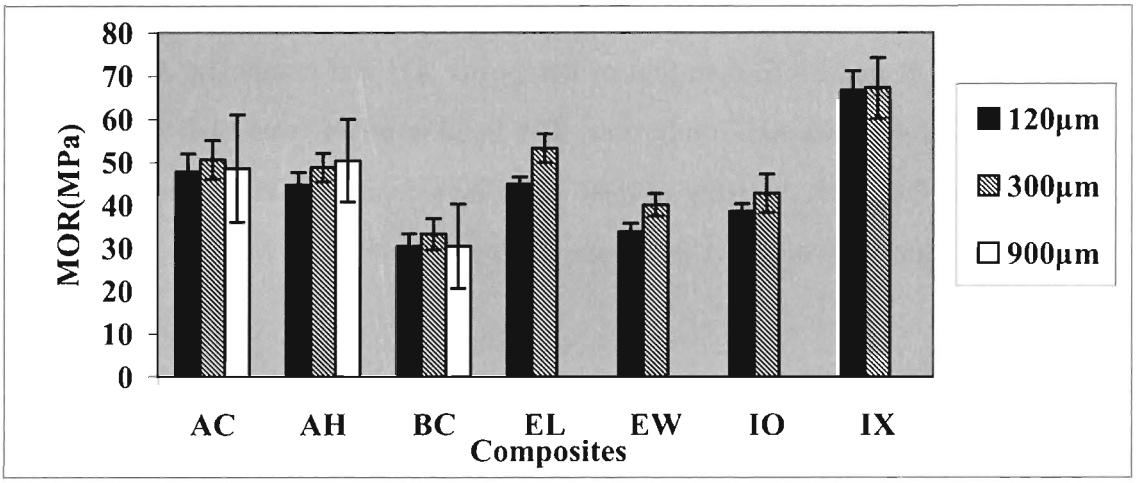

Figure 3.3. Effects of fiber length on MOR of composites with 80 wt% fiber content and 20 wt% plastic content; Error bars represent standard deviation. *Filled bars*, *Filled bars*, Cellulose fiber length=120μm; *shaded bars*, Cellulose fiber length=300μm; *open bars*, Cellulose fiber length=900μm

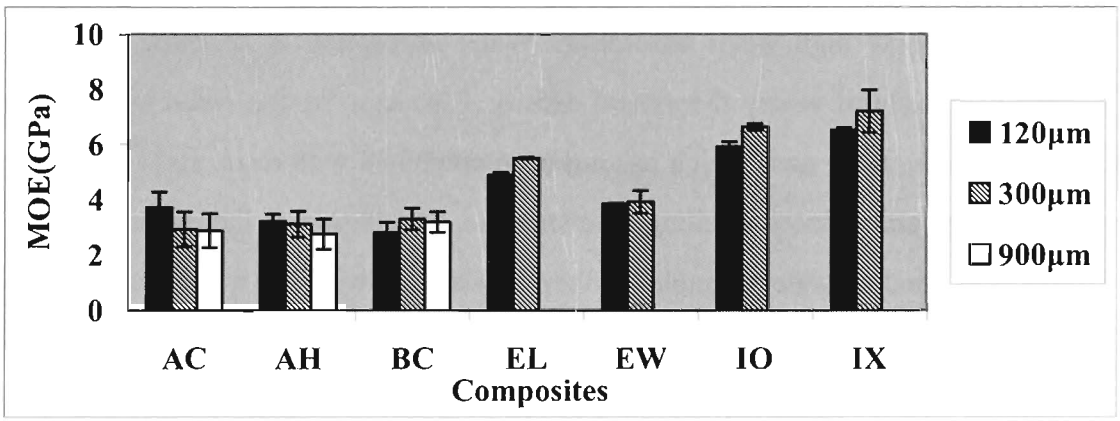

Figure 3.4. Effects of fiber length on MOE of composites with 80 wt% fiber content and 20 wt% plastic content; Error bars represent standard deviation. *Filled bars*, *Filled bars*, Cellulose fiber length=120μm; *shaded bars*, Cellulose fiber length=300μm; *open bars*, Cellulose fiber length=900μm

Effect of method A, method B, injection and extrusion molding

Widthwise extrusion composite (EW) had a lower MOR and MOE than that of lengthwise extrusion composite (EL). Injection mold without lubricant (IX) had a higher MOR and MOE than that of injection mold with lubricant (IO). Composite BC had lower MOR and MOE than that of composite AH and composite AC because of low density of AC and AH composites. The volume of BC was high with plenty of voids, and as the result, bonding of resin and fibers decreased. However, the injection mold without lubricant of 80 wt% PP gave the highest MOR and MOE.

3.3.2 Water absorption

Effect of fiber content

Method A: As shown in Figures 3.5 and 3.6, water absorption increases as the resin content decreases. It is expected that water absorption takes place at the first approximation permeating a void portion and secondly as the binding water of cellulose. Therefore, the molded composite having a density much different from theoretical density may show high water absorption. Water absorption is accepted also in the molded composite of nearly theoretical density. This may be explained by that water permeates through the part, which has not been combined with resin, stays as cellulose binding water and induces swelling of composite. In addition to the expansion due to the cellulose binding water a tangle of fiber is destroyed with the water that permeated into the composite. Therefore, expansion of the molded composite is large with composites of more water absorption. The thickness swelling increases as the resin content decreases.

Method B: Water absorption increases as the resin content decreases. This composite is porous and contains many void spaces. Since the composite contains many voids, much water is absorbed. Ratio of water absorption to the theoretical void (measured density/theoretical density) showed a parallel tendency. Since the composite did not absorb water completely in the experimental conditions of keeping in water for 24 hours,

it is expected to be similar with a method A molded composite in that water has permeated between fibers, and so on as above. The thickness swell increases as the decrease of resin content. The factor controlling thickness swelling is the same as a method A molded composite. Therefore, a composite with much water absorption shows high expansion, and so on.

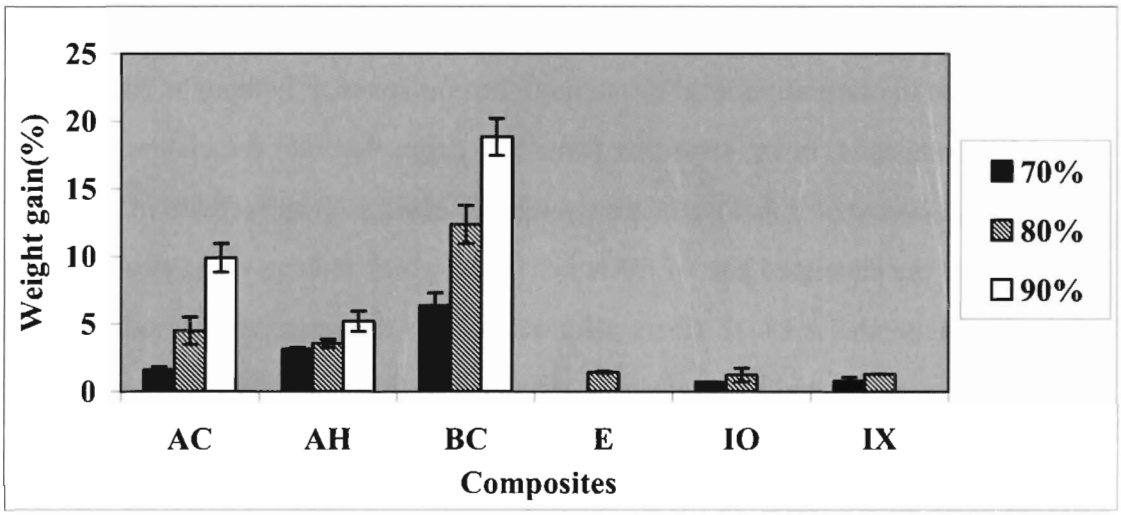

Figure 3.5. Effects of fiber content on weight gain of composites with 300μm cellulose. Error bars represent standard deviation; *Filled bars*, Cellulose/PP/MAPP=70/28/2; *shaded bars*, Cellulose/PP/MAPP=80/18/2; *open bars*, Cellulose/PP/MAPP=90/8/2

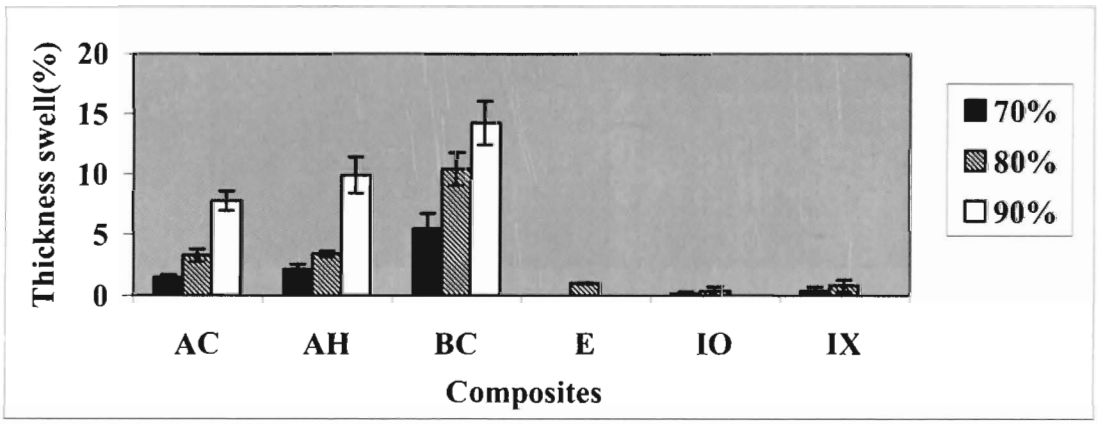

Figure 3.6. Effects of fiber content on thickness swell of composites with 300μm cellulose. Error bars represent standard deviation. *Filled bars*, Cellulose/PP/MAPP=70/28/2; *shaded bars*, Cellulose/PP/MAPP=80/18/2; *open bars*, Cellulose/PP/MAPP=90/8/2

Effect of fiber length of cellulose

Figure 3.7 implies the trend in weight gain of increasing fiber length of cellulose, while Figure 3.8 represents the thickness swell of the increasing fiber length of cellulose. Composite of 120 μm of fiber length has the low swell per 1 wt% of water absorption. Since fiber length is short, tangles between fibers have less developed. Water absorption is near to theoretical ratio of void, but since water absorption for 24 hours in water has not reached to the saturation level throughout the composite, it is thought, like a method A molded composite, in the state that water has permeated into the clearance between fibers. It is also observed that water absorption increased with an increase in fiber length. Therefore, as the entangled part of fibers increases, which induces more clearance in the composite, a bonded part of fibers with resin may decrease. A method A molded composite has little void. Therefore, it is expected that water has permeated and is absorbed by the fiber that has not been bonded with resin. In this case, this part may increase with longer fiber, and consequently, water absorption is high. The thickness swell increases as the fiber length become long. A tangle of a fiber may have been destroyed with the permeated water, water binding to cellulose may increase and composite expands. Therefore, a longer fiber with many tangles between fibers may show high expansion.

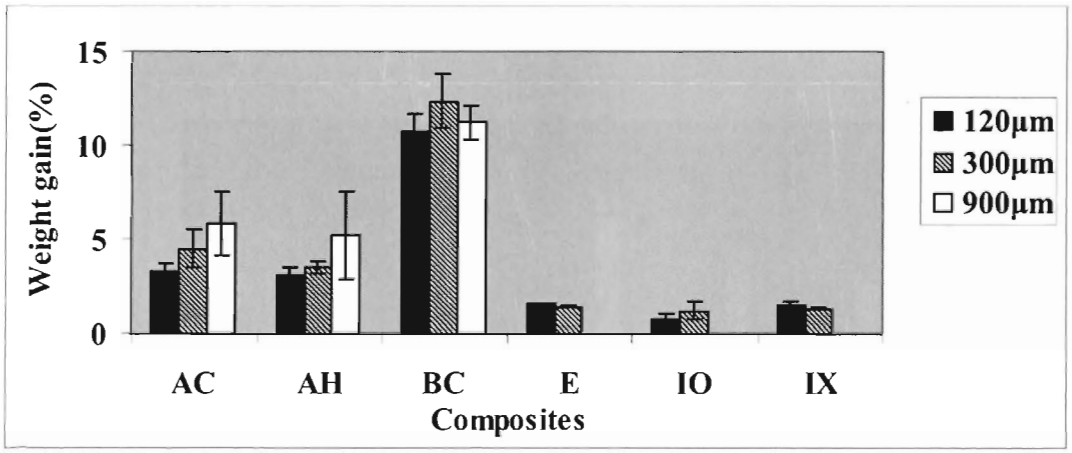

Figure 3.7. Effects of fiber length on weight gain of composites with 80 wt% fiber content and 20 wt% plastic content. *Filled bars*, *Filled bars*, Cellulose fiber length=120μm; *shaded bars*, Cellulose fiber length=300μm; *open bars*, Cellulose fiber length=900μm

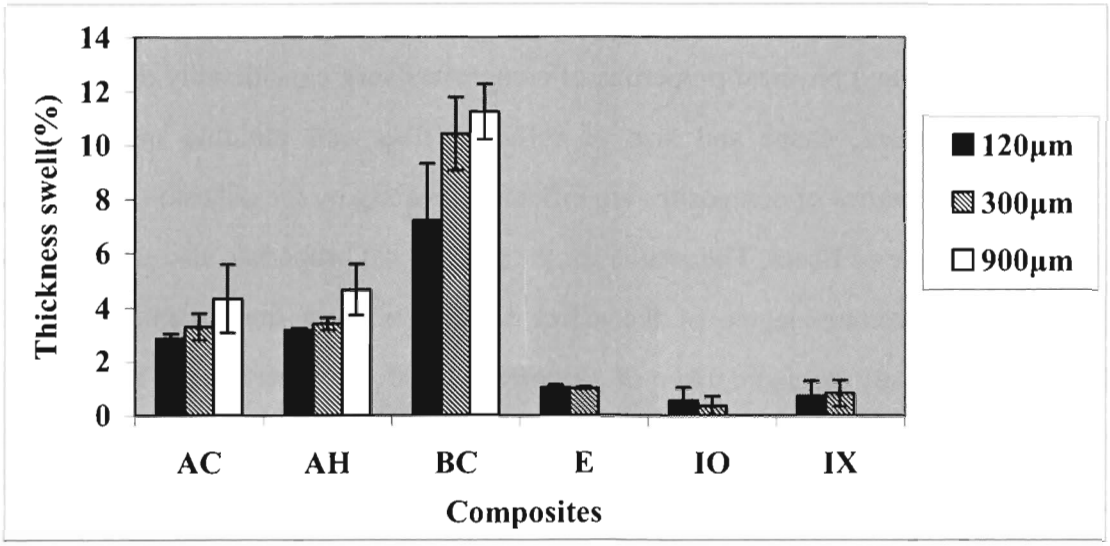

Figure 3.8. Effects of fiber length on thickness gain of composites with 80 wt% fiber content and 20 wt% plastic content. *Filled bars*, *Filled bars*, Cellulose fiber length=120μm; *shaded bars*, Cellulose fiber length=300μm; *open bars*, Cellulose fiber length=900μm

Effect of method A, method B, injection and extrusion molding

A method A molded composite has little water absorption and expansion compared with a method B molded composite. The difference is explained on the basis of density difference and void ratio of chapter 4. For the composites of 70 wt% cellulose content, thickness swelling per 1 wt% of water absorption is larger with method A composite than method B composite. Since the composite of 70 wt% cellulose content is abundant in fiber, there are few fibers that are not covered with resin. Therefore, when there are many voids inside of the composite, cellulose/PP/MAPP composite of high density tends to expand more by water absorption. Injection molded samples show the least water absorption. The values obtained for water absorption in injection molded composite with lubricant and without lubricant lies near by. Although micrographs do not show a clear difference at preset, more coverage of fiber by resin will be expected for injection molded composites.

3.4 Conclusions

The mechanical and physical properties of composites vary considerably depending on the plastic content, shape and size of cellulose fiber and molding methods. The mechanical properties of composites are influenced mainly by the adhesion between the matrix and tangle of fibers. The results for the mechanical properties also supported the existence of a certain degree of the effect of miscibility in the composite plastics. Because of loosely arranged fiber of composites, 900 μm fiber length and 90 wt% plastic content composites had the highest absorption of water resistance among the composites. The trend of water resistance and mechanical properties is injection mold >extrusion mold>compression mold by method A>compression mold by method B. We concluded that injection and extrusion molded composites, of cellulose in PP with MAPP, gave the best mechanical properties and physical properties.

3.4 Conclusions

The mechanical and physical properties of composites vary considerably depending on the plastic content, shape and size of cellulose fiber and molding methods. The mechanical properties of composites are influenced mainly by the adhesion between the matrix and tangle of fibers. The results for the mechanical properties also supported the existence of a certain degree of the effect of miscibility in the composite plastics. Because of loosely arranged fiber of composites, 900 μm fiber length and 90 wt% plastic content composites had the highest absorption of water resistance among the composites. The trend of water resistance and mechanical properties is injection mold >extrusion mold>compression mold by method A>compression mold by method B. We concluded that injection and extrusion molded composites, of cellulose in PP with MAPP, gave the best mechanical properties and physical properties.

CHAPTER4

Density and Morphology of Cellulose/Polypropylene/MAPP Composites

4.1 Introduction

The increased interest in the use of wood as filler and/or reinforcement in thermoplastics is also due to low density [27]. Reducing the weight of wood plastic composites is another challenge for these materials. The density of wood plastic composites is almost twice that of solid lumber [28]. The main drawbacks are the difficulties of achieving good dispersion and strong interfacial adhesion between the hydrophilic wood and the hydrophobic polymers which leads to composites with rather poor durability and mechanical properties [27]. Therefore density and morphological properties were studied in this chapter.

4.2 Experimental method

4.2.1Composite density

Composite density of the samples was determined using composites molded by compression, injection and extrusion molding. The composite density was calculated according to the following equation as the average of twelve specimens:

Density of composite =Weight of composite/ (Length×Width×Thickness)

4.2.2 Morphology of composites

Microscope images of cellulose fibers of fiber length 120, 300 and 900 μm and the fractured surfaces after mechanical testing were taken using Moritex Inf 500 DA at different magnifications.

4.3 Results and discussion

4.3.1Composite density

Effect of fiber content

Figure 4.1 presents the variations of composite density of different plastic content of compression, injection and extrusion molding. For composite prepared by Method A, when the fiber content is 80 wt% or more, the density of a hammer mill compound is higher than that of a cutter mill compound probably because the relative difference of component reinforcements, their aspect ratio and also the extent of chemical modification during milling influences the overall rheological behavior. Fluidity is low when the fiber content is high. Since fluidity is high at 70 wt% of fiber content indicates there may be influences of the pulverization method on the densities of composites. No remarkable relationship is observed between the fiber content and product density. Method A composite is prepared under a press condition setup for bringing the density close to the theoretical density. Therefore, all press pressures and press times differ. When the fiber content is low, theoretical density is attained by low pressure and a short press time. However, high pressure is needed when the fiber content is high. In this case, a compound of low fluidity would be crushed during the molding process. If the fiber shape will be changed during the molding process, the fiber content may have influence on various performances. In this context, press molding has merit that can be applied for a wide range of molding conditions. Therefore, a wide range of fiber contents was selected for making composites of compression molding.

For composite prepared by Method B, density of composite also decreased with increase in cellulose content. Hence, the void ratio of these composites would be increasing with increasing fiber content. A possible explanation for the voids is movement of air from within the cell lumen to the cell wall-PP interface during compaction [29]. Again, fluidity of compound is high when the fiber content is low. Since method B molding is carried out under the constant press conditions, a compound

of high fluidity is expected to give a more compact composite. The melt-flow characteristic is peculiar for each formulation and can be estimated, since the technique used in this experiment gives little influence, except for flow characteristics, on the various product performances.

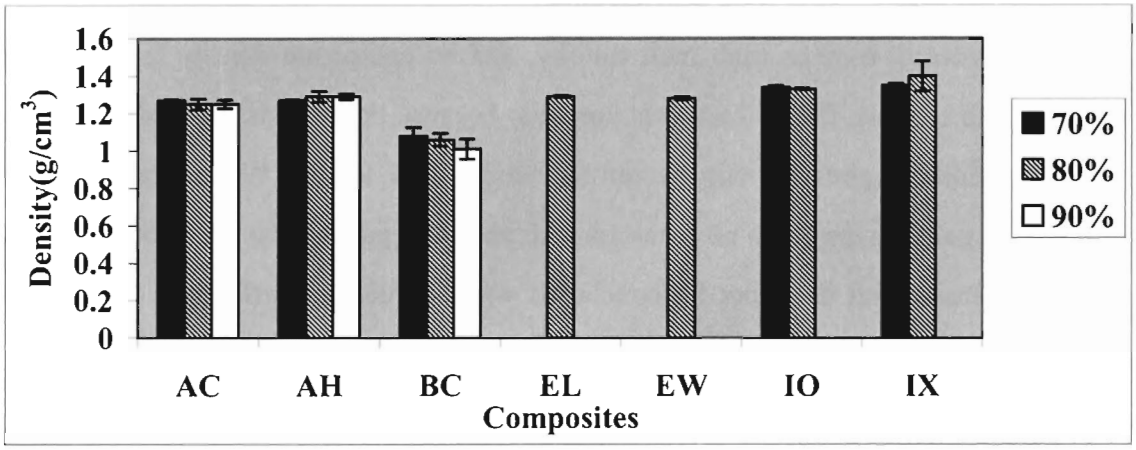

Figure 4.1. Density (g/cm^3) of composites with different fiber content of 300μm cellulose; Error bars represent standard deviation. *Filled bars*, Cellulose/PP/MAPP=70/28/2; *shaded bars*, Cellulose/PP/MAPP=80/18/2; *open bars*, Cellulose/PP/MAPP=90/8/2

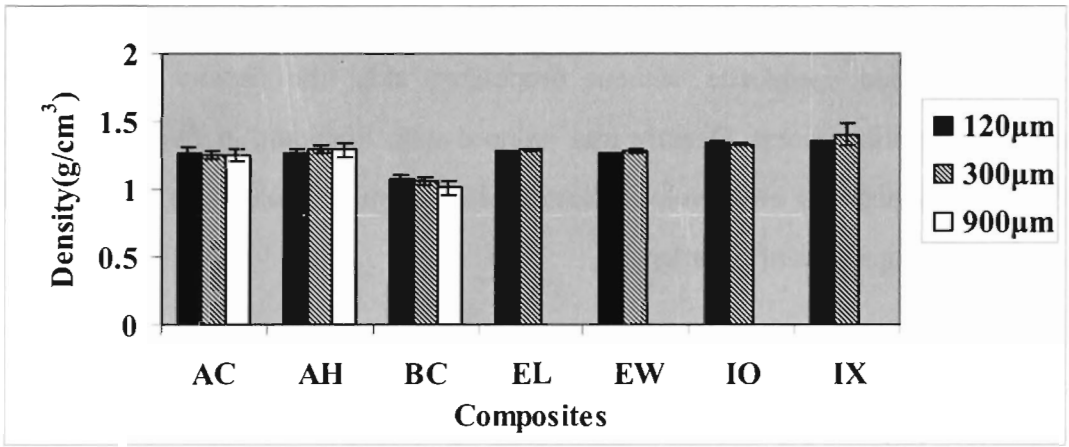

Figure 4.2. Density (g/cm^3) of composites with different fiber lengths of 80 wt% fiber content and 20 wt% plastic content. *Filled bars*, *Filled bars*, Cellulose fiber length=120μm; *shaded bars*, Cellulose fiber length=300μm; *open bars*, Cellulose fiber length=900μm

Effect of fiber length of cellulose

Figure 4.2 presents the density of composites of different fiber length of 80 wt% fiber content of compression, injection and extrusion molding. A hammer mill produces more fine powder than a cutter mill. Therefore, when fiber length is long, compound is more finely powdered, ensures high melt fluidity, and so composite density is high. When fiber length is short, this influence is not clear because the fiber is originally small and fine. In addition, packing may be influenced by fiber length. When fibers are long, maximum packing may also be accessed with optimum particle size distribution leading to high density, but it cannot be concluded with the density difference of this level. Composite density decreases when fiber length becomes increased.

Effect of compression, injection molding and extrusion molding

There is a tendency that the particle size of a hammer mill compound is smaller than that of a cutter mill compound. As the result, an aspect ratio becomes larger for cutter mill fiber. For this reason, the compound with the same resin content may show low fluidity and give the density difference of the composites AH and AC. In case of injection molded composite without processing aids, the density decreases with increasing plastic content. Density was reduced with lubricant, at fiber content of 80 wt%, hence processing aid developed some void. Similar observation was observed in the case of comparison of fiber length.

Effect of fiber content on the morphology of the fracture surfaces

Charge-coupled device (CCD) micrographs of fractured surfaces of compression molded composite containing 30%, 20%, and 10% PP are shown in Figure 4.3. As the fiber content increased, more fluff of fiber was detected. The occurrence of fluff is considered to be a starting point of fracture. This observation is more pronounced with composites of high fiber content, so it is assumed that strength of the composite is maintained by tangles between fibers. As the fiber content increased, more fiber

ball-like material was observed on the fracture surface. In composite with 70% cellulose, the fiber was dispersed into the matrix and coated with PP. For the composite containing 90% cellulose, a fibrous particle of cellulose was partially covered by the PP, with part of the surface still not covered. This proves that a fully developed interfacial interaction was not developed in the 90% cellulose composite.

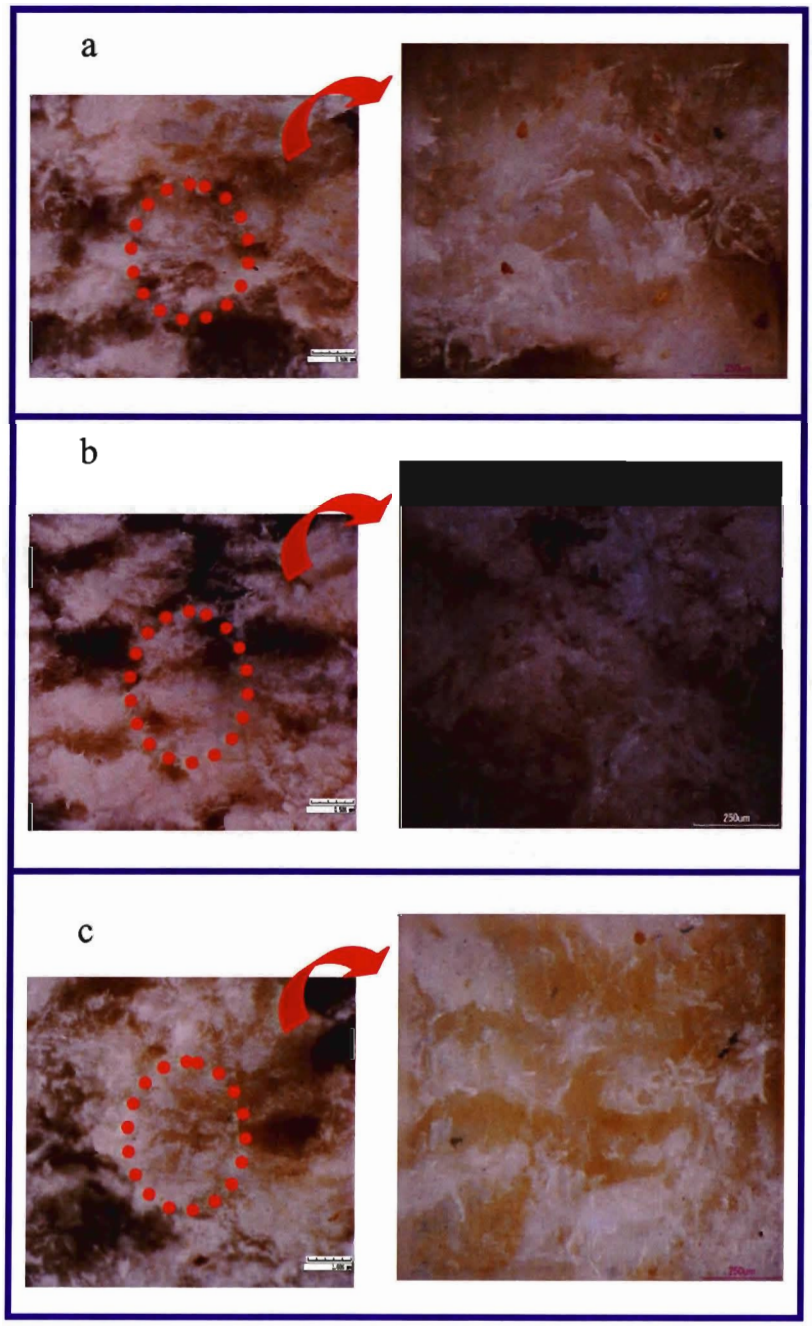

Figure 4.3. Micrographs of fractured surfaces of compression molding composites containing cellulose of 300μm fiber length; *a*, Cellulose/PP/MAPP=70/28/2; *b*, Cellulose/PP/MAPP=80/18/2; *c*, Cellulose/PP/MAPP=90/8/2

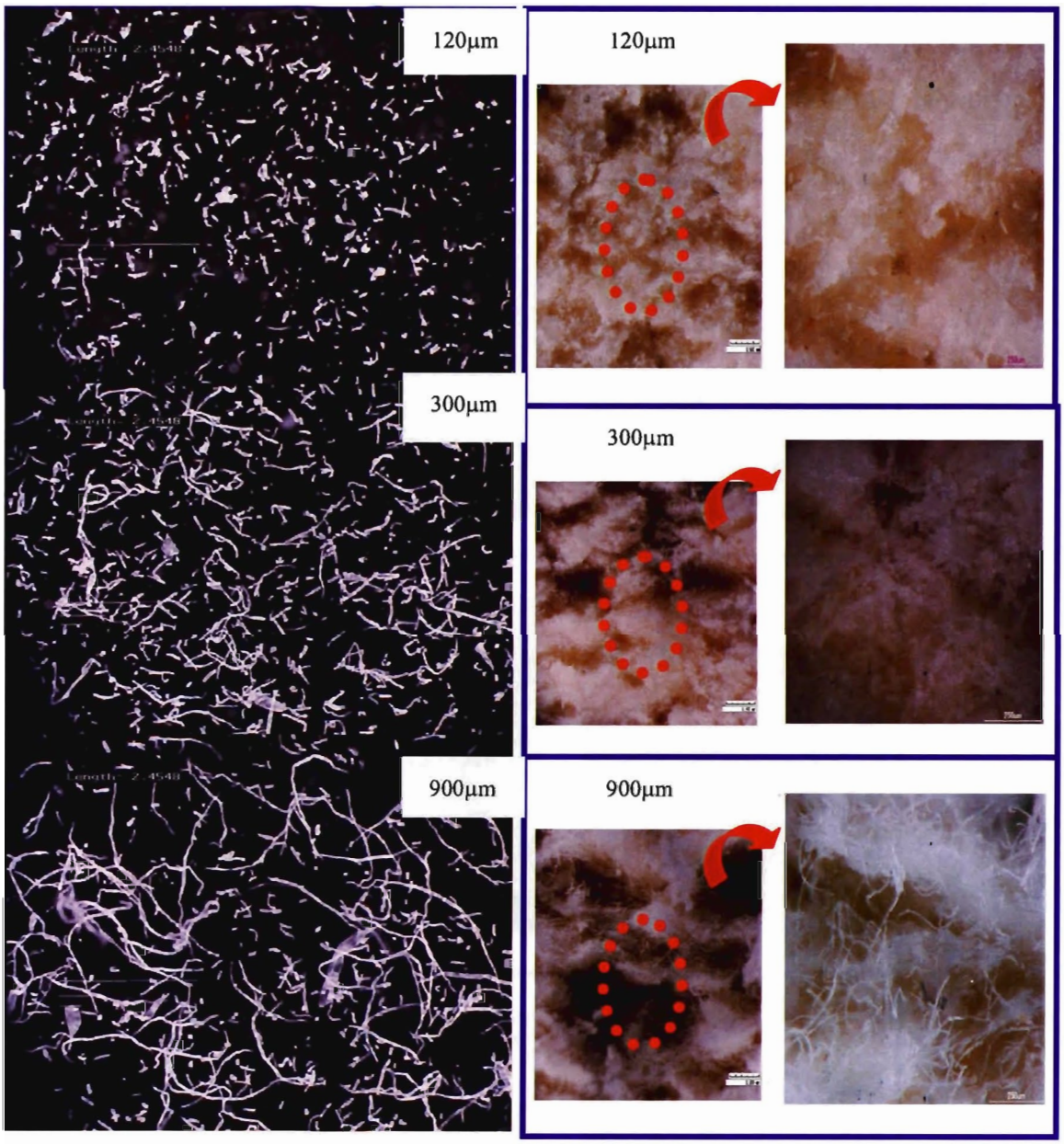

Figure 4.4. Micrographs of **a)** cellulose fibers of 120µm, 300µm and 900µm length, and **b)** fractured surfaces of compression molded composites containing cellulose fibers of 120µm, 300µm and 900µm length

Effect of cellulose fiber length on the morphology of the fracture surface

Microscope images of cellulose fiber and fractured surfaces of compression-molded composite with increasing fiber length of cellulose are shown in Figure 4.4. When long fibers were present, they were conspicuous on the fracture surface. A stratified pattern was conspicuous on fracture surfaces when fibers were long. Fracture of composites took place at weak parts of the composite where fibers were not well bonded with resin. Fluff was more conspicuous for composites with long fibers. On other hand, lamination also occurred when fibers were long. This phenomenon should have some influence on the strength. The cellulose fibers with fiber lengths of 120, 300, and 900μm partially changed into micro particles during melt-extrusion processing. In the case of 120μm fibers, homogeneity of the blended mixture was observed, indicating that it should serve as a good filler of polymer matrix.

Effect of compression, injection, and extrusion molding

Micrographs of fractured surfaces of extrusion moldings and injection moldings are shown in Figure 4.5. The interfacial interactions were limited in the compression-molding composites, probably because of a smaller number of ester bonds between highly fibrous cellulose and the MAPP/PP matrix [30,31]. The micrographs of extrusion-molded composites EW No. 1 composition (120μm fiber length, 80% cellulose) clearly show gaps and voids in the PP matrices as well as along the cellulose fibers, the surfaces of which are smooth and practically intact, and that there exist some aggregates of cellulose fibers. Much improved distribution of particles of cellulose was found in the injection molding with lubricant IO and without lubricant IX with 120μm fibers and 80% cellulose. The micrographs also reveal a marked improvement in interfacial adhesion between cellulose particles and the MAPP/PP matrix, which was brought about by increased surface area. The fiber was not uniformly dispersed in the melted PP matrix

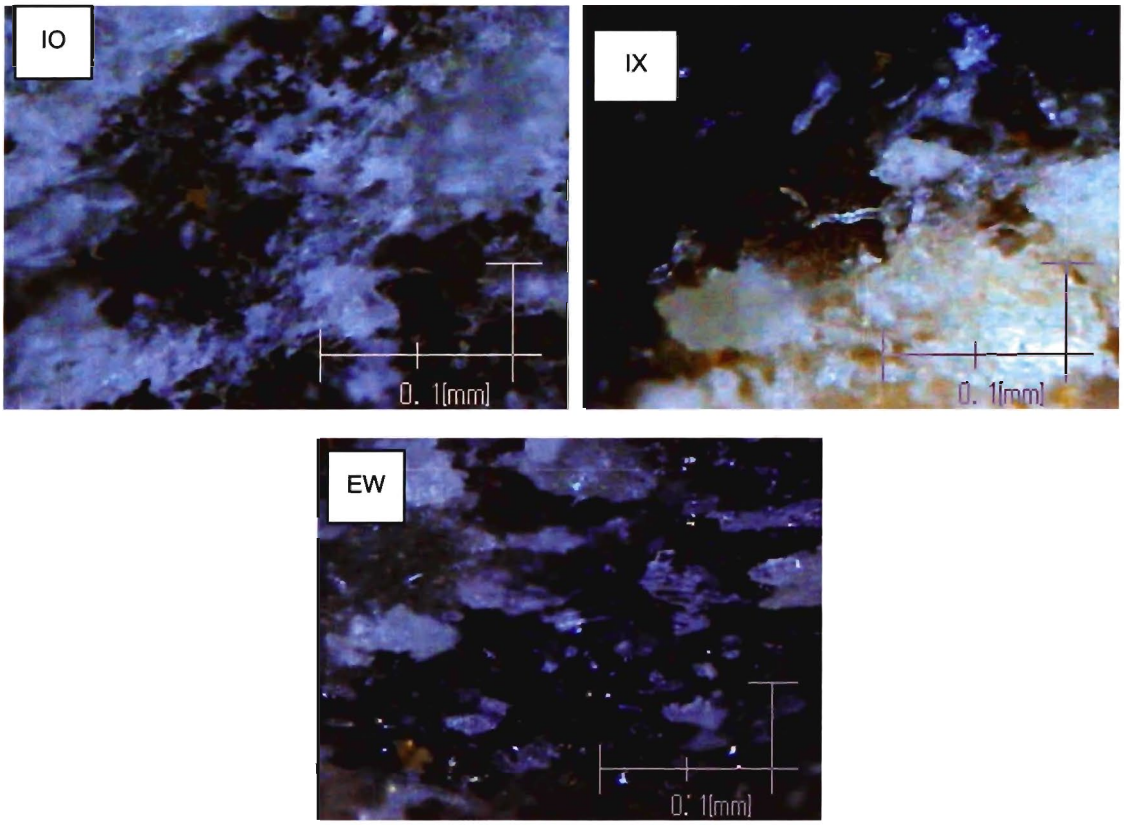

Figure 4.5. Micrographs of fractured surfaces of extrusion molding and injection molding composite with 80 wt% fiber content and 20 wt% plastic content. *IX*, Injection mold without lubricant; *IO*, Injection mold with lubricant; *EW*, Extrusion mold sample in widthwise direction

Conclusions

This study focused on composite density comparison and evaluation of the morphology of cellulose/polypropylene/MAPP composite. The composite of small fiber showed good compatibility and adhesion between the plastic and the cellulose fiber, while the composites of long fiber showed poor adhesion between the two phases. Extrusion allows better mixing of cellulose, thermoplastic and additives because of the high shear of extrusion processing, as shown by CCD micrographs.

CHAPTER 5

Thermal Mechanical Analysis and Dynamic Thermal Mechanical Analysis of Cellulose/Polypropylene/MAPP Composites

5.1 Introduction

Thermal mechanical analysis helps in gathering information on the stress transfer and helps explaining the reasons for the property changes [2]. WPC are stiffer and have much lower thermal expansion than plastics and absorb less moisture than wood, and they are also more brittle than plastics and offer lower strength, stiffness, and creep resistance than solid wood [32].

The glass transition temperature (T_g) is one of the most important and representative parameters of the chemical and physical properties of polymer matrix composite materials. T_g can be correlated to the mechanical properties of a composite material, to the chemical structure of its matrix and to the materials performance under specific environmental conditions [33]. All solid materials expand almost linearly (in every direction) with increasing temperature and contract with decreasing temperature. It is this degree of expansion–contraction that can make the phenomenon an unpleasant one, and at the same time challenging for designers with plastic and composite. DMTA supplies an oscillating force, causing a sinusoidal stress to be applied to a sample, which generates a sinusoidal strain. By the measurement of the magnitude of the deformation at the peak of the sine wave and the lag between the stress and strain waves, properties such as the modulus, viscosity, and damping can be calculated. The five regions of viscoelastic behavior typical of a thermoplastic polymer are presented in Figure 5.1. The glass-transition range is characterized by a sharp decrease in the elastic modulus of the polymer and is dependent on the state of the polymer and its thermal properties. In an effort to simplify the determination of T_g, it is commonly defined as the maximum of the damping ratio, E''/E' (tan δ), or the maximum of E''. Several researchers, however, have found that a more accurate determination can be derived from the onset of the

change in the slope of the E' curve. The effects of fiber size and polymer content on the thermal, dynamic and mechanical behavior of cellulose/polypropylene/MAPP composites are presented in this chapter.

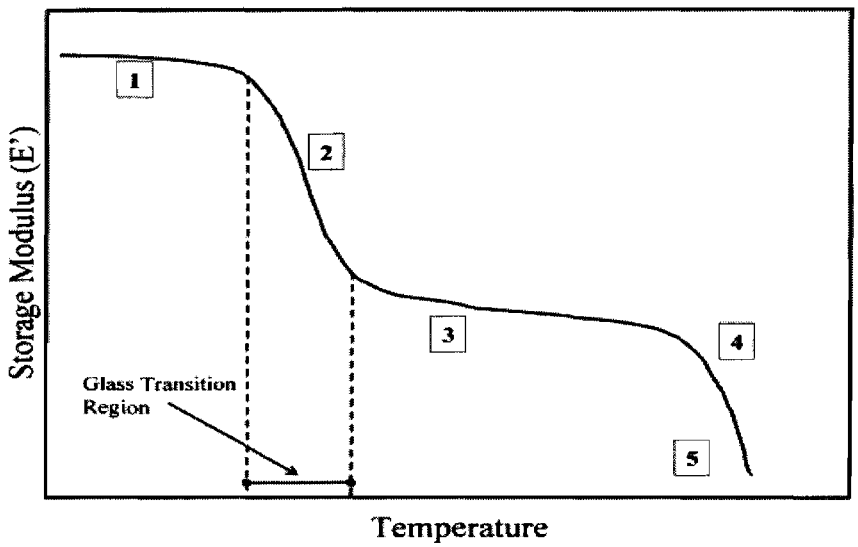

Figure 5.1. Five regions of polymer viscoelastic behavior. *(1)* glassy region; *(2)* glass-transition region; *(3)* rubbery region; *(4)* rubbery flow region; and *(5)* liquid flow region

5.2 Experimental Method

5.2.1 Dynamic mechanical thermal analysis

The dynamic mechanical data were obtained with a Rheology DVE-V4 dynamic visco-elastic analyzer. Samples were tested at 1 Hz in the temperature range 50°C to 250°C with a heating rate of 3°C/min under air. The specimen size was 30×6×2mm (length×width×thickness). The viscoelastic parameters, that is, the mechanical loss factor (damping) tan $\delta = E''/E'$ (E' and E'' are storage and loss moduli, respectively) and E', were recorded as a function of temperature. The dynamic forces were 30N (sine wave y=1.25sin θ).In this experiment a sinusoidal load is applied to the material. A sinusoidal motion, inducing either stretching or bending was applied to the sample.

Analyzed samples were; neat PP and composites molded by compression, extrusion and injection molding.

5.2.2 Thermal mechanical analysis

Thermal mechanical analysis of the materials as a function of temperature was measured using Thermo-mechanical analyzer (TMA) SS6100 (Seiko Instruments, Tokyo). The heating rate was 3°C /min over a temperature range of 10°C to 50°C. The specimen dimension was 10×5×2mm (length×width×thickness). A coefficient of thermal expansion (CTE) was measured for one material over the temperature range of 20°C to 30°C.

5.3 Results and Discussion

5.3.1 Dynamic mechanical thermal analysis

Effect of fiber content

Dynamic mechanical thermal analysis (DMTA) gives information on storage E' and loss E'' moduli, and the dissipation factor ($\tan \delta = E''/E'$). DMTA can give knowledge about the interface between wood/cellulose and polypropylene matrix. The DMTA were performed on various composites of different fiber content in tensile mode. Analyzed samples were; neat PP and composites with 90%, 80%, 70%, cellulose. The storage modulus at 50°C for the different samples is plotted in Figure 5.2. As can be seen in Figure 5.2, the neat PP showed lowest modulus. For all molding processes, addition of cellulose increased the modulus significantly. The injection molding without lubricant composites (IX) showed high modulus compared to injection molding with lubricant (IO). Lubricant thus has a negative effect on storage modulus during DMTA experiments. It is evident from the Figure that the modulus is highest for AC composite of 80% cellulose. In case of IX, modulus of the composites is less affected by fiber content. While modulus decreases with increasing fiber content for AH and IO. The

increase in storage modulus indicates enhanced adhesion between the filler and matrix, leading to an interphase of higher stiffness.

As reported by Lai et al. [34] tan δ broadens and the peak position shifts if there is an interaction between the matrix polymer and the filler/reinforcement. In Figure 5.3, the peak position of tan δ of the analyzed composites is plotted. It can be seen in Figure. 5.3, there is no significant shift in the peak position of tan δ towards a higher temperature when cellulose is added to the plastic (PP). A further increase or decrease in the peak position towards higher temperatures would be expected for the composites compared to neat PP when PP was mixed with others in a molecular level. A small increase in the tan δ peak was observed for AH and IX composite containing 80% cellulose. On the other hand, no increase in the tan δ peak was observed in remaining composites indicating no practical change of matrix in composites.

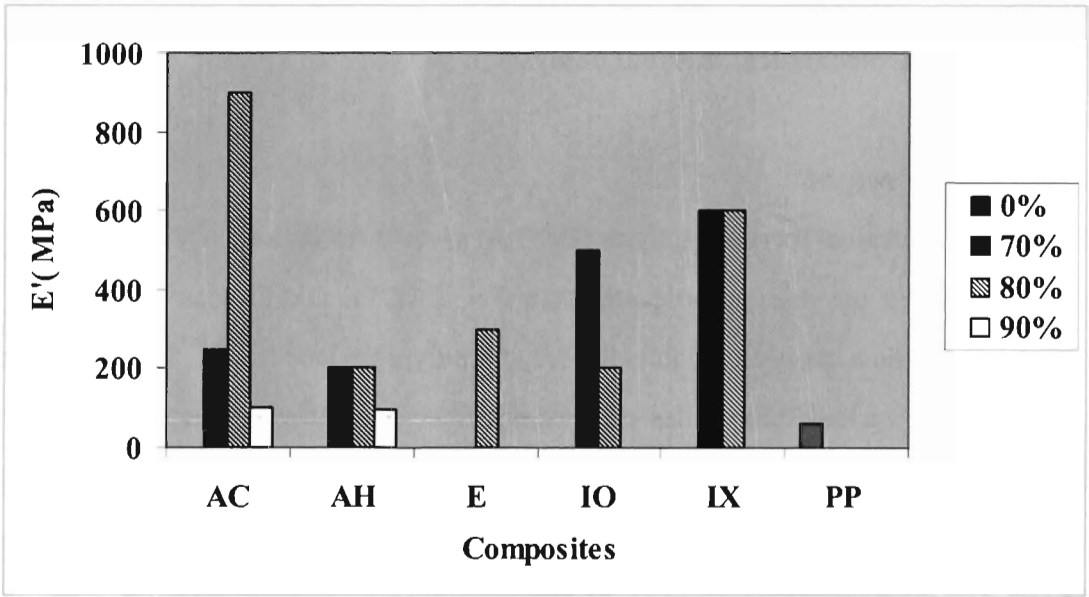

Figure 5.2. Effects of resin content on the storage modulus of composites with 300μm cellulose at 50°C. *Filled bars*, Cellulose/PP/MAPP=70/28/2; *shaded bars*, Cellulose/PP/MAPP=80/18/2; *open bars*, Cellulose/PP/MAPP=90/8/2; *gray bars*, PP

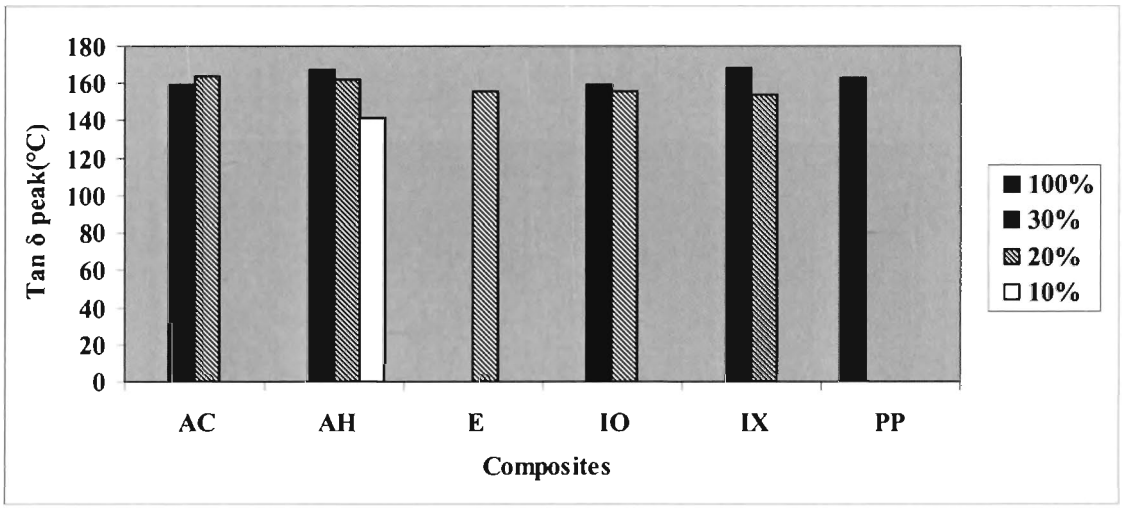

Figure 5.3. The peak position of tan δ of composites with different fiber lengths of 80 wt% fiber content and 20 wt% plastic content. *Filled bars*, Cellulose/PP/MAPP=70/28/2; *shaded bars*, Cellulose/PP/MAPP=80/18/2; *open bars*, Cellulose/PP/MAPP=90/8/2; *gray bars*, PP

Effect of fiber length

The cellulose/PP/MAPP composites containing 120, 300, and 900μm cellulose fiber length were selected for investigating the effects of fiber length of cellulose on the composite properties. The results of the DMTA analysis shown in Figure 5.4 are storage modulus of composites with different fiber length of cellulose. For composite AC, it can be seen that the modulus slightly increased to a maximum value for composite containing 120μm. The effect of fiber length was more pronounced for the composite AH. In case of AC, AH, and IO the modulus tended to decrease with increasing fiber length. On other hand, modulus increases with increasing fiber length for composite E. The tan δ peak (Figure. 5.5) decreases when fiber length of cellulose increases in most of the cases. This is expected because the decrease in peak indicates that the number of mobile segments involved has increased indicates more flexible polymer matrix. This may also indicate the formation of fiber ball for longer fiber, leaving a matrix of increasing homogeneity. Furthermore, the tanδ peak position of composite AC containing 120μm is shifted a little toward a higher temperature. The shift in the tanδ

peak also shows that the molecular motion is restricted, and this confirms the strong interaction between the cellulose and PP/MAPP

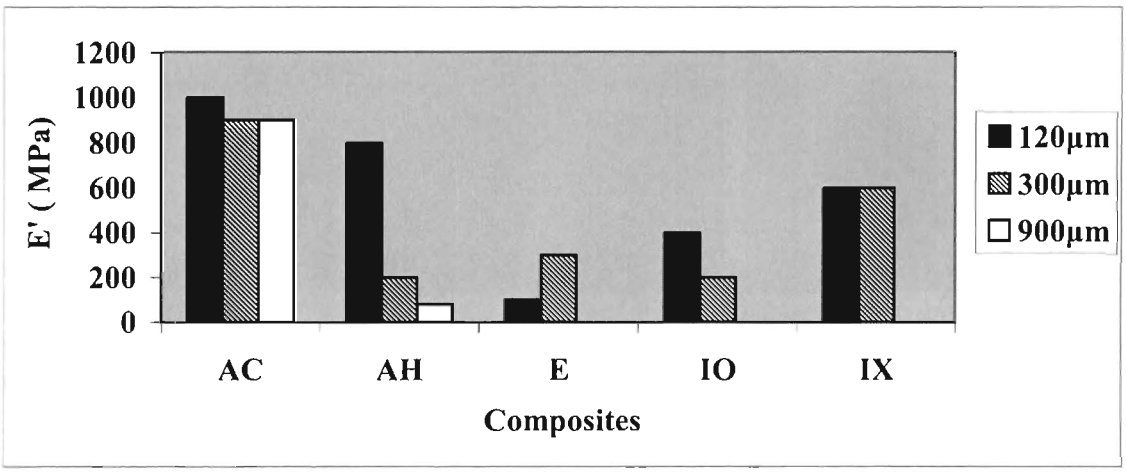

Figure 5.4. Effects of fiber length on storage modulus of composites with 80 wt% fiber content and 20 wt% plastic content at 50°C. *Filled bars*, *Filled bars*, Cellulose fiber length=120μm; *shaded bars*, Cellulose fiber length=300μm; *open bars*, Cellulose fiber length=900μm

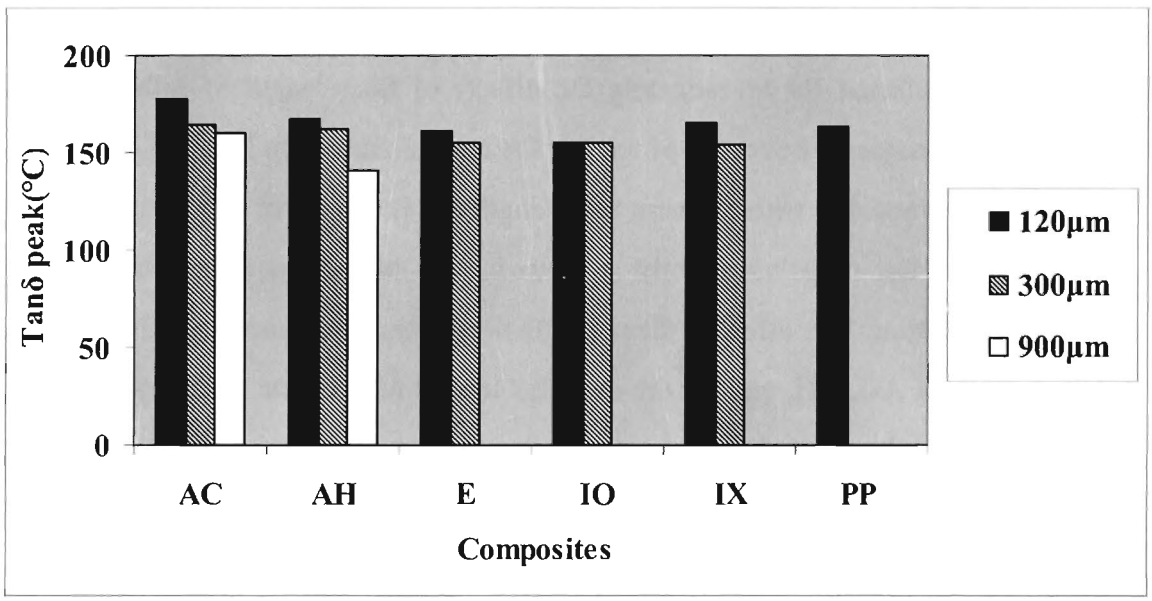

Figure 5.5. The peak position of tan δ of composites with different resin content of 300μm cellulose. *Filled bars*, *Filled bars*, Cellulose fiber length=120μm; *shaded bars*, Cellulose fiber length=300μm; *open bars*, Cellulose fiber length=900μm

Effect of compression, injection, and extrusion molding

The dynamic mechanical analysis of neat PP and composites was carried out from 50 to 250°C at 1Hz. The loss modulus *E″* is the viscous response of viscoelastic materials. It is a measure of the energy dissipated or lost as heat per cycle of sinusoidal deformation, when different systems are compared at the same strain amplitude.

Figure 5.6 presents the storage modulus (*E′*) as a function of temperature for neat PP and the composites AC, AH, E, IO and IX with 30% PP/MAPP of fiber length 120μm. At low temperatures, *E′* values of AC, AH, IX and IO are very close to each other. It is an indication, that, at low temperatures the fibrils do not contribute much in imparting stiffness to the composite. In the case of all composites there is a sharp fall in *E′* on passing through the glass transition temperature (T_g). It is due to the increased molecular mobility of the polymer chains above T_g. There is a large fall in modulus with increasing temperature for PP in comparison with other composites, the stiffness at high temperature being determined by the amorphous regions, which are very submissive above glass transition temperature. Four different transitions were observed in case of PP, the transition between 140 and 160°C and the transition between 160 and 180°C. The latter transition could be subdivided in two sub transitions between 180 and 190°C and between 190 and 205°C. Extrusion molding and Injection molding composites (E, IO, and IX) have four clear transitions, whereas compression molding composites did not show clear transitions. From last transition temperature, the points did not follow a clear trend because of the deformation of the material due to high temperatures next to the melting point. Every transition implied a change in the decreasing slope of the log *E′*, which indicated that the blends became more viscous in nature with rising temperature.

In the Figure 5.7, variation of dissipation factor (tan $\delta = E''/E'$) with temperature for neat PP and composites at 1 Hz is shown. The ratio of loss modulus to storage modulus is measured as the mechanical loss factor or tan δ. The damping properties of the material give the balance between the elastic phase and viscous phase in a polymeric structure. The damping behavior of the composites in the transition region is governed

by a) mechanical relaxation of the matrix and the fiber themselves b) relaxation of the interface between the fiber and the matrix c) fiber loading and fiber length. It is interesting to study the behavior of the composites at the α relaxation. The peak heights of the composites are less than that of PP. It can be attributed to the higher storage modulus values of these composites at this temperature. There is a negative shift in the T_g of PP phase for the composites in comparison with neat polymer. T_g for neat PP is 163.3°C and for IX and AC it is 164.2°C. For the composites IO, ET, H8I, and H10I, T_g is 155.4, 155.4, and 162.1°C respectively. The shift in T_g in the case of IX and AC is marginal (0.9°C) when compared to neat PP. This result indicates interfacial interaction is poor at this draw ratio. This fact is consistent with the interpretation of the storage modulus curve. Every transition implied a change in the decreasing slope of the log *E′* curve and the increase in the tan δ, which indicated that the polymer became more viscous in nature with rising temperature.

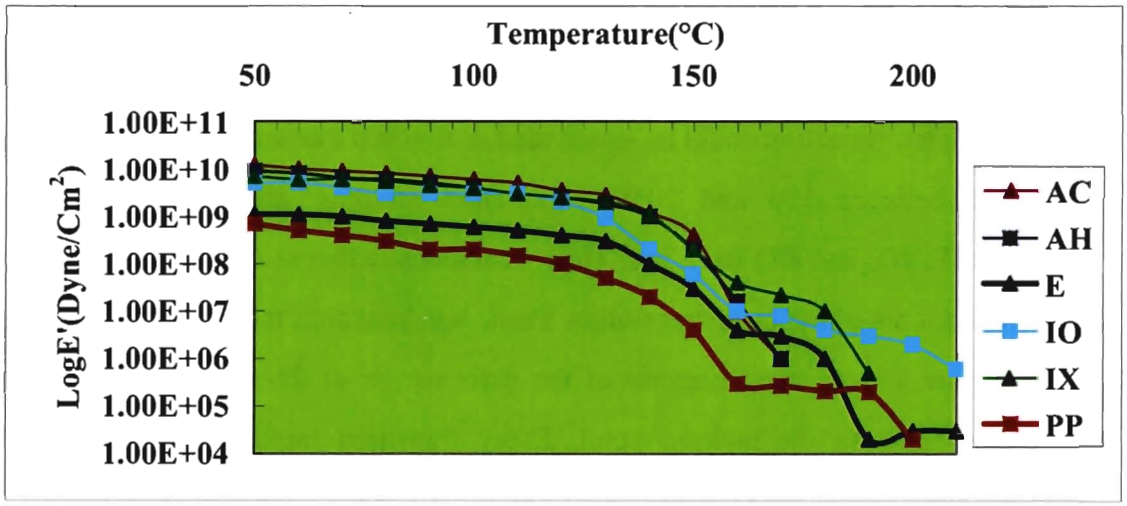

Figure 5.6. The storage modulus (*E′*) as a function of temperature of composites with 120μm fiber length cellulose and 80/20 cellulose/PP/MAPP ratio

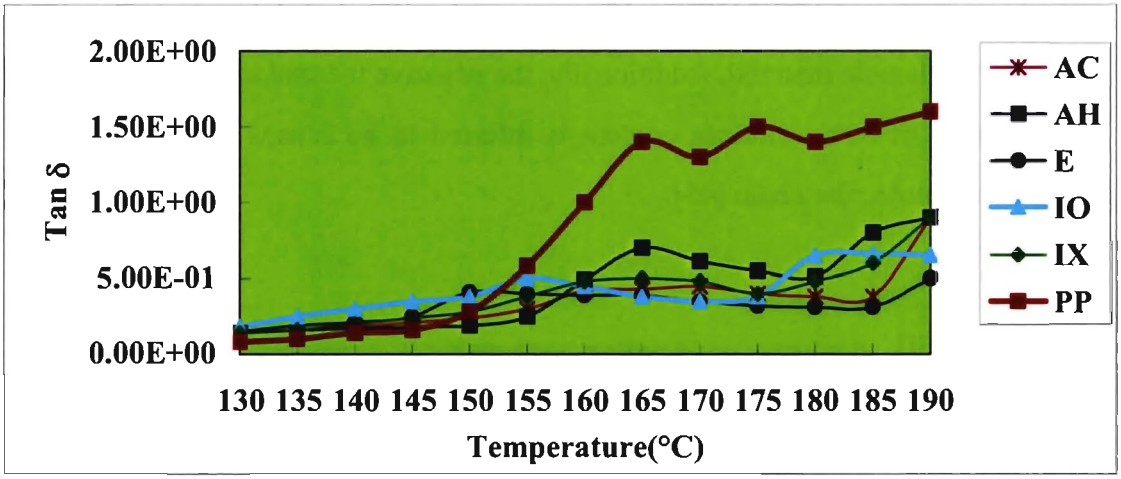

Figure 5.7. The variation of tanδ as a function of temperature of composites with 120μm fiber length cellulose and 80/20 cellulose/PP/MAPP ratio

5.3.2 Thermal mechanical analysis

Effect of fiber content

Figure 5.8 shows the coefficient of thermal expansion (CTE) of AC, AH, BC, E, IX, IO composites containing different fiber content. The CTE for each specimen was calculated according to the well-known formula:

$$CTE = \Delta L / L_0 \Delta T$$

Where ΔL is the change in length (mm), ΔT is the change in temperature (°C), and L_0 is the initial composite length (mm).

The thermal stability of the materials shows that as the plastic content increases, CTE increases as well. It is well known that the CTE of the low molecular weight polypropylene is greater than the cellulose polymeric matrix, and thus with increase of plastic content in the formulations, the CTE of the resulting cellulose plastic increases. The presence of plastic limits the crystallinity in the matrix and increases the free

volume present in the system. Thus, increasing the amount of plastic in the formulation gives a more flexible material. Additionally, the negative thermal expansion coefficients IX composite of 80% cellulose content is inferred to be caused by the reduction of length of the molecular chain [45].

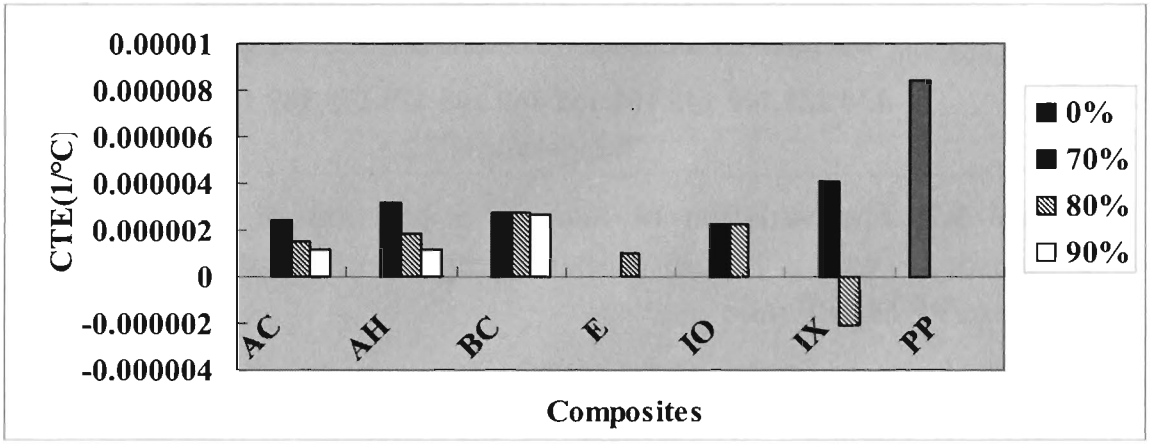

Figure 5.8. The coefficient of thermal expansion (CTE) of composites with different fiber content of 300μm cellulose. *Filled bars*, Cellulose/PP/MAPP=70/28/2; *shaded bars*, Cellulose/PP/MAPP=80/18/2; *open bars*, Cellulose/PP/MAPP=90/8/2; *gray bars*, PP

Effect of fiber length

Figure 5.9 shows the effect of the fiber length of cellulose on the CTE of AC, AH, BC, E, IO and IX composites. Composite of short fiber exhibited the higher CTE, whereas long fiber showed lower CTE of these composites. The CTE depends upon the type of bonding between the constituent molecules/atoms, and is larger for van der Waals-type than for covalent type bonded solids.

Effect of compression, injection, and extrusion molding

For neat PP, the coefficient of thermal expansion (CTE) is about twice as much compared with cellulose/PP/MAPP composites, which are 70% filled with cellulose. The amount of filler affects the value of CTE. Fibers are tightly squeezed in the matrix during mold cooling because of which the fiber poses a mechanical restrain on the

opening of the polymer chain during heating and thus reduce the overall CTE of the composite. Surface of the wood fiber acted as an additional nucleating site for the formation of crystallite of PP matrix therefore enhancing the crystallinity of the matrix as revealed from the DMTA results of the cellulose/PP/MAPP composite. The increased crystallinity would pack the matrix more densely thus resulting in reduction of CTE. This can be another identifiable reason for the reduction of CTE of a crystalline polymer like PP when filled with cellulose fiber [35].

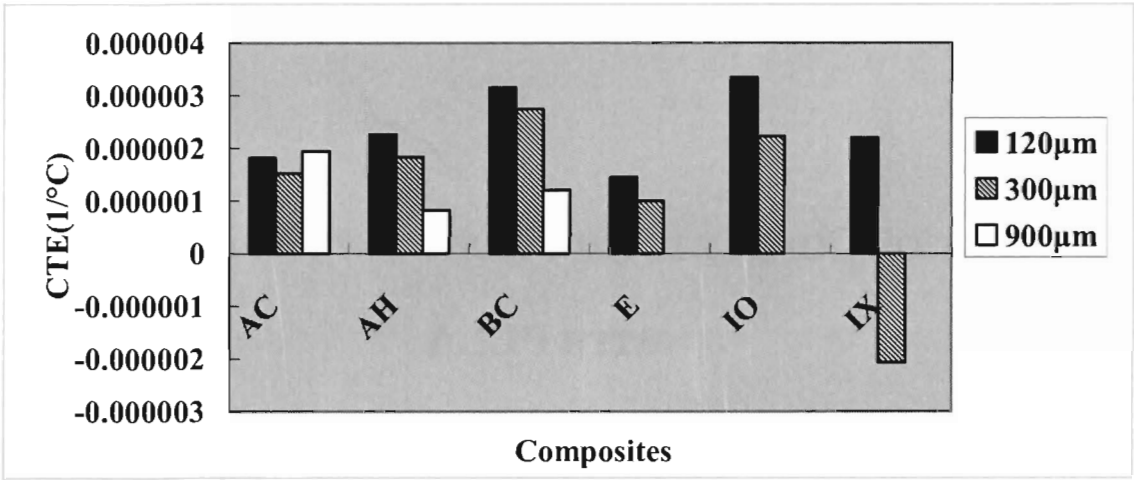

Figure 5.9. The coefficient of thermal expansion (CTE) of composites with different fiber lengths of 80 wt% fiber content and 20 wt% plastic content. *Filled bars*, *Filled bars*, Cellulose fiber length=120µm; *shaded bars*, Cellulose fiber length=300µm; *open bars*, Cellulose fiber length=900µm

Conclusions

Biofiber-plastic composite of cellulose and polypropylene were fabricated using compression, extrusion and injection molding. Different compositions of the composites were characterized by dynamic thermal mechanical analysis and thermal mechanical analysis, Wood fiber embodied in PP matrix gave an appreciable rise in storage modulus. Coefficient of linear thermal expansion (CTE) of composites was uniformly reduced with the fiber reinforcement.

PART 2

STUDY OF COMPLETE BIOPLASTIC BY REPLACING PP WITH PLLA

CHAPTER 6

Synthesis and Characterization of Modified Poly (L-lactic acid)

6.1 Introduction

Composite materials from the annually renewable natural fibers and biodegradable matrices have been developed in the past decade in an attempt to find alternatives to the fossil fuel-based polymeric materials in the automotive and packaging industries. Biodegradable polymers are very attractive from an environmental standpoint, but there are practical difficulties associated with their use. For example, the brittleness and high water absorption of poly (lactic acid), a polymer derived from corn, limits its potential applications. Researchers are investigating methods for the preparation of modified poly (lactic acids) that are tougher and still retain environmentally beneficial characteristics. Several research groups have reported the modification of biodegradable polymer (like poly lactic acid, polycaprolactone etc.) by maleic anhydride [36, 37]. Cai et al. used different silk fibroin samples to modify poly (D, L-lactic acid) surfaces [38]. Nagasawa et al. investigated the most effective crosslinking agent triallyl isocianurate for modifying poly(lactic acid) by irradiation technique [39]. Recently, synthetic rubbers were even-blended with poly (lactic acid) to improve impact strength while bearing in mind the restriction that only a limited quantity of petroleum based materials could be added to retain its biodegradable nature. The aim of this chapter is synthesis and characterization of PLLA with γ-butyrolactone(BL), ε-caprolactone(CL) and hydroxypivalic acid(HA). CL monomer is considered to have potential for modifying PLLA due to their low molecular weight. Therefore, modification of PLLA by ε-Caprolactone (CL) was examined in detail with a Lewis acid catalyst of hafnium (IV) chloride and $Sn(Oct)_2$ (tin(II) bis(2-ethylhexanoate))

6.2 Experimental Method

6.2.1 Materials

The 99% ε-caprolactone (b.p=96-97.5°C, density1.03g/ml at 25°C) and 98% hafnium chloride were purchased from Aldrich and all were used without further purification. The 99% γ-butyrolactone(density 1.132g/ml at 20°C) and hydroxypivalic acid(2,2-Dimethyl -3-hydroxypropionic acid, m.p=123-127°C) were supplied by Wako pure chemical industries Ltd. The commercial grade of PLLA (PL002,Tensile strength=59MPa, elongation at break=2%, Modulus of elasticity=3040MPa, T_m=171 °C, T_g=57°C) was obtained from Kuraray, Japan.

Table 6.1. Composition and reaction condition of copolymerization

PLLA (g)	Monomer (1ml)	Catalyst (0.1g)	Reaction Time	Resulting Copolymer
5	CL	$HfCl_4$	5day	P(LA-co-CL)
5	HA	$HfCl_4$	3day	P(LA-co-HA)
5	BL	$HfCl_4$	2day	P(LA-co-BL)

6.2.2 Synthesis of PLLA

The copolymers were obtained by synthesis of PLLA with CL, BL, and HA are summarized in Table 6.1. The reactive modification of PLLA was carried out in a three neck flask under nitrogen atmosphere and 100 rpm by sequentially mixing with mechanical stirrer (with catalyst). Reaction condition, catalyst and amount of PLLA and monomer were listed in Table 6.2.

Table 6.2. Composition and reaction condition of copolymerization of PLLA with ε-caprolactone

No.	PLLA (g)	CL (ml)	Catalyst (0.1g)	Temperature (°C)	Reaction Time (Hr)
1	5	1	$HfCl_4$	180	24
2	5	2	$Sn(Oct)_2$	180	24
3	2	6	$HfCl_4$	120	3
4	2	6	$HfCl_4$	120	6
5	2	6	$HfCl_4$	120	24

6.2.3Gel permeation chromatography

Molecular weights were compared by gel permeation chromatography (GPC) using a Shimadzu Liquid Chromatograph LC10AD equipped with a Gelpack® column operating at room temperature and employing SPD-10A Shimadzu UV VIS detector with universal calibration. Chloroform was used as the solvent at a flow rate of 1 ml/min.

6.2.4 Proton nuclear magnetic resonance

The structure of the PLLA and copolymers were analyzed by proton nuclear magnetic resonance (1H-NMR) spectra. 1H-NMR spectra were measured with a Nippon. Denshi JEOL FT-270 NMR at 25°C using deuterated chloroform as the solvent.

6.2.5 Matrix assisted laser desorption/ionization time-of-flight mass spectrometry

The PLLA copolymerized with CL (P(LA-co-CL)) were also characterized by matrix assisted laser desorption/ionization time-of-flight mass spectrometry (MALDI-TOF MS) was performed using the Waters MALDI micro MX mass spectrometer using a

337 nm nitrogen laser. To 1μl of the sample solution was added 1μl of the matrix solution and 1μl was deposited on a plate and air-dried prior to load into the mass spectrometer. The matrix solution of dithranol was prepared with 20 mg/ml in tetrahydrofuran.

6.2.6 Differential scanning calorimetry

Thermal analysis was carried out by means of differential scanning calorimetry (DSC) using a TA instrument, DSC2190 differential scanning calorimeter and TA instrument, thermal analyst 2000. For DSC, copolymer samples of 5–10mg in weight were heated at 10°C /min under a nitrogen atmosphere over a temperature range of 60 to 250°C in order to observe their glass transition (T_g), crystallization (T_c) and melting (T_m) temperatures.

6.3 Results and discussion

6.3.1 Gel permeation chromatography

Molecular weights, and the distributions, of the synthesized copolymers P (LA-co-CL), P (LA-co-BL), and P (LA-co-HA) were compared with gel permeation chromatography (GPC). GPC chromatograms of resulting copolymers are shown in Figure 6.1. It was found that gel permeation chromatograph molecular weight (MW) of P(LA-co-BL) and P(LA-co-CL) are almost same as PLLA while MW of P(LA-co-HA) decreased. Regarding the molecular weight distribution, bimodal distribution was observed in case of P(LA-co-BL) and P(LA-co-CL), but unimodal distribution was appeared in case of P(LA-co-HA). Upon exposure to heat and water, the polymer breaks down to low molecular weight oligomers.

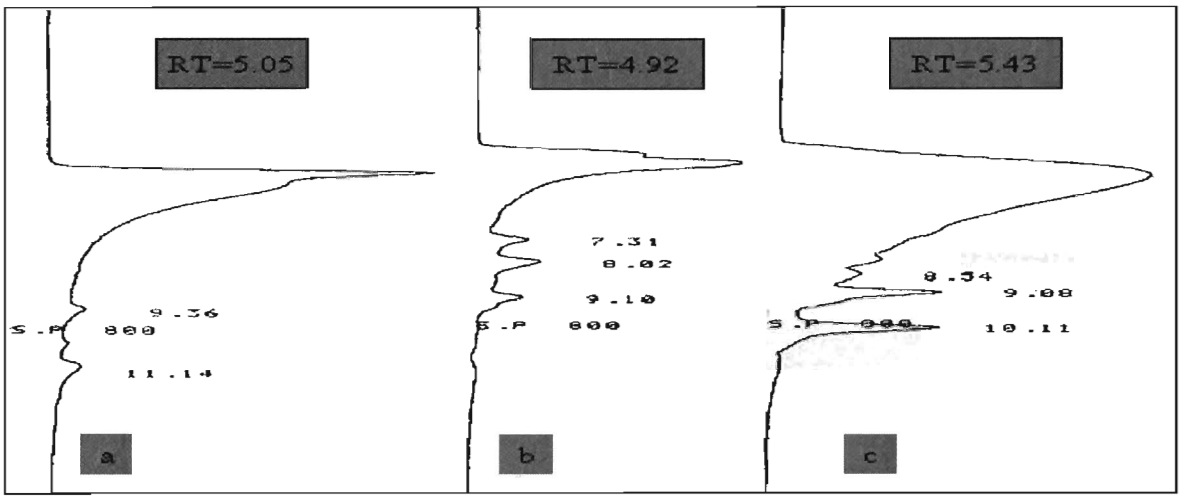

Figure 6.1 GPC chromatographs of the copolymers synthesized from PLLA and monomers *(a)* P(LA-co-CL); *(b)* P(LA-co-BL); *(c)* P(LA-co-HA); *RT* Retention time

6.3.2 Proton nuclear magnetic resonance

After GPC analysis, CL monomer is considered to have potential for modifying PLLA. Therefore, modification of PLLA by CL was examined in detail. All copolymers listed in table were analyzed by proton NMR. All of the NMR spectra exhibited peaks of the hydroxyl CH and the methyl CH_3 proton of PLLA and peaks of $CH_2CH_2CH_2CH_2CH_2$ proton of CL, example of which is shown in Figure 6.2 for copolymer No. 1 and 3. The hydroxyl CH and the methyl CH_3 proton of PLLA were identified at around 5.1-5.3ppm and 1.5-1.7ppm, respectively. Proton NMR spectrum of CL shown on Figure 6.2(b) has peaks at approximately 4.1ppm, 2.3ppm and 1.9-2.0ppm with relative intensities in ratio 1:1:3, respectively. The end groups of the copolymers were identified and the composition of PLLA and CL of the copolymers were determined from their 1H-NMR spectra by ratioing the peak areas corresponding to the PLLA methyne protons at 5.0–5.3ppm and the CL e-methylene protons at 3.9–4.2 ppm. The calculated compositions (LA:CL mol%) are given in Table 6.3 and are all seen to be within 18% change of the initial PLLA and CL feeds, as would be expected since the copolymerization was taken to near quantitative conversion. As typical examples, the 1H-NMR spectra of copolymer No. 1 and 3, as shown in Figure 6.2, clearly show how

the peak areas corresponding to the PLLA protons increase relative to those of the CL protons.

Table 6.3. Chemical compositions, repeating unit, and mass range of the copolymers P(LA-co-CL) listed in Table 6.2

No.	PLLA/CL	Repeating Unit	Mass range	PLLA/CL by NMR
PLA	PLA	LA	350-1600	
1	83/17	LA	350-2200	91/9
2	71/29	LA	450-2200	74/26
3	25/75	CL	350-1800	35/65
4	25/75	CL	350-2200	32/67
5	25/75	CL	350-2200	7/93

6.3.2 Proton nuclear magnetic resonance

After GPC analysis, CL monomer is considered to have potential for modifying PLLA. Therefore, modification of PLLA by CL was examined in detail. All copolymers listed in table were analyzed by proton NMR. All of the NMR spectra exhibited peaks of the hydroxyl CH and the methyl CH_3 proton of PLLA and peaks of $CH_2CH_2CH_2CH_2CH_2$ proton of CL, example of which is shown in Figure 6.2 for copolymer No. 1 and 3. The hydroxyl CH and the methyl CH_3 proton of PLLA were identified at around 5.1-5.3ppm and 1.5-1.7ppm, respectively. Proton NMR spectrum of CL shown on Figure 6.2(b) has peaks at approximately 4.1ppm, 2.3ppm and 1.9-2.0ppm with relative intensities in ratio 1:1:3, respectively. The end groups of the copolymers were identified and the composition of PLLA and CL of the copolymers were determined from their 1H-NMR spectra by ratioing the peak areas corresponding to the PLLA methyne protons at 5.0–5.3ppm and the CL e-methylene protons at 3.9–4.2 ppm. The calculated compositions (LA:CL mol%) are given in Table 6.3 and are all seen to be within 18% change of the initial PLLA and CL feeds, as would be expected since the

copolymerization was taken to near quantitative conversion. As typical examples, the 1H-NMR spectra of copolymer No. 1 and 3, as shown in Figure 6.2, clearly show how the peak areas corresponding to the PLLA protons increase relative to those of the CL protons.

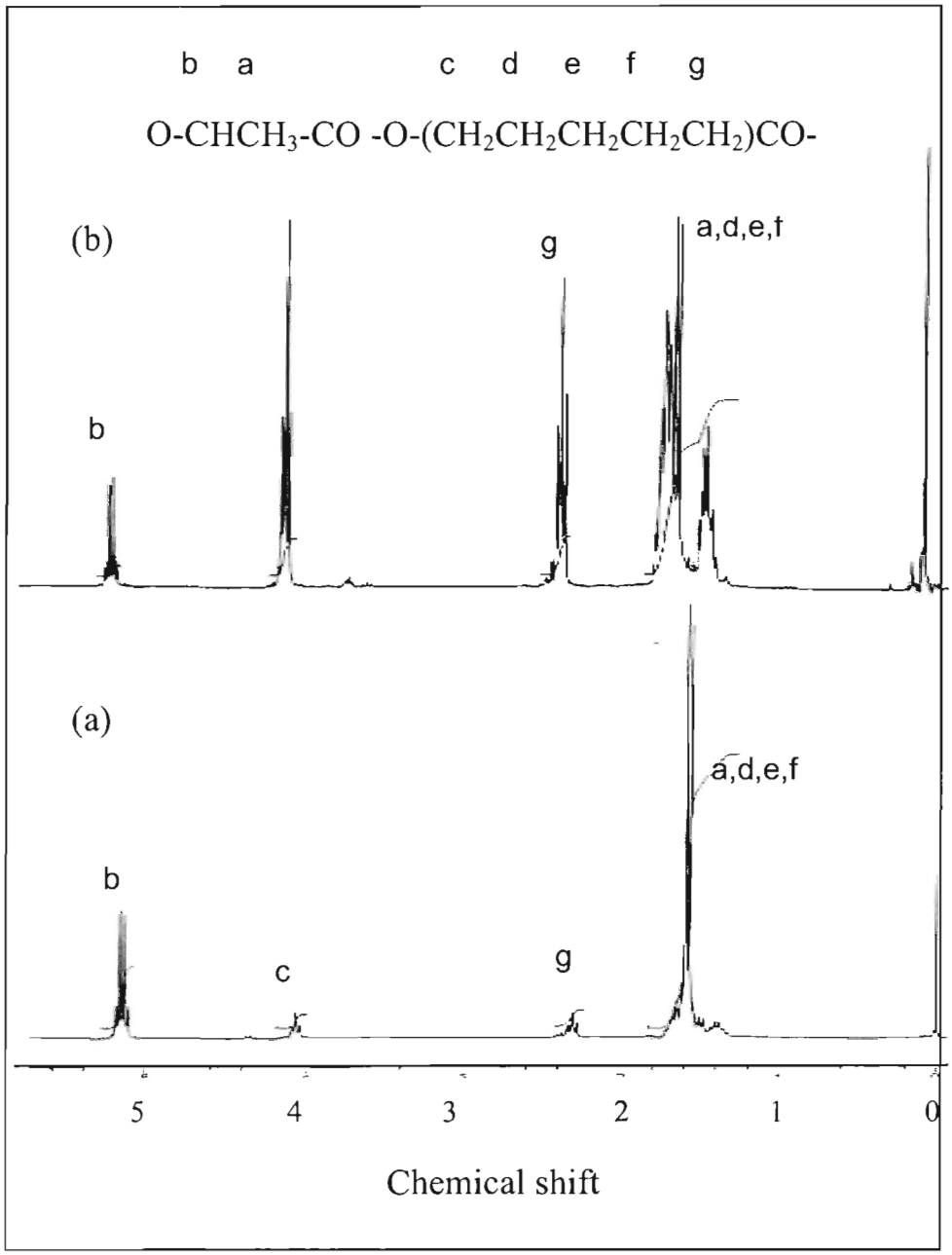

Figure 6.2 1H-NMR spectra recorded in $CDCl_3$ as solvent at room temperature *(a)* P(LA-co-CL) No. 1;*(b)* P(LA-co-CL) No.3 listed in Table 6.2

6.3.3 Matrix assisted laser desorption/ionization time-of-flight mass spectrometry

In order to study each individual species in a mixture of oligomers matrix-assisted laser desorption ionization time-of-flight mass spectrometry (MALDI-TOF MS) can be employed, as it possesses unprecedented high sensitivity allowing for desorption and ionization even of very large molecules such as polymer samples [40]. Figure 6.3 shows the MALDI-TOF MS mass spectrum, acquired in linear mode, of the P(LA -co-CL) copolymer (No.1 listed in Table 6.2). This mass spectrum showed the distribution of molecular weight centered around 1000 g/ mol for copolymer, 400 to 2000m/z. The intense peaks in Figure 6.3 are the sodium cationized oligomers, differing by 72 m/z that correspond to the repeating unit of the open-chain polymer. These peaks correspond, respectively, to the masses of lactic acid and CL units. The total molar mass of each major peak is given by the sum of the individual contributions from, the multiple n of the PLLA repeat unit (72.06g/mol), $HOCH_3$ (55g/mol), $[O\text{-}(CH_2)_5CO]_2$ (228.28 g/mol), and sodium (23.00 g/mol) (the small deviation of 2 a.m.u. is within the MALDI-TOF MS accuracy of +4 a.m.u.) [40].

Figure 6.4 shows the MALDI-TOF MS mass spectra, recorded in linear mode, of selected fractions of P (CL-co- LA) copolymer (No.3 listed in Table 6.2). Each spectrum shows a unimodal distribution of ions, centered at 1000m/z, 400 and 1800. The total molar mass is given by the sum of the individual contributions the multiple n of the CL unit and H $[O\text{-}CHCH_3\text{-}CO]_3$ - OCH_3 complexed with Na., i.e. 2 to 12.

Table 6.4 contains the ion assignment. The most abundant ions can be assigned to sodium-cationized linear copolymer chains.

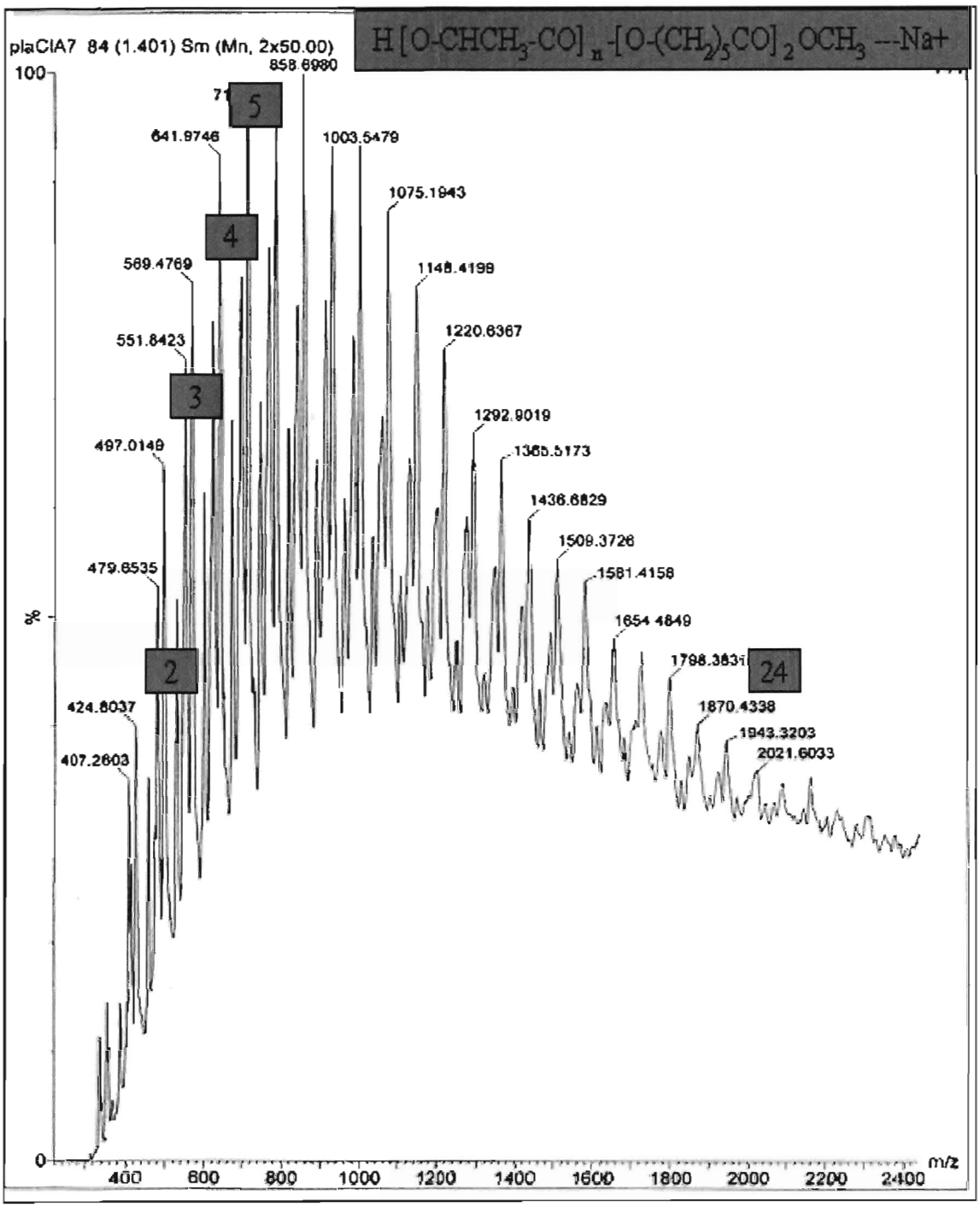

Figure 6.3 MALDI-TOF mass spectrum of Copolymer No.1 derived from PLLA and CL

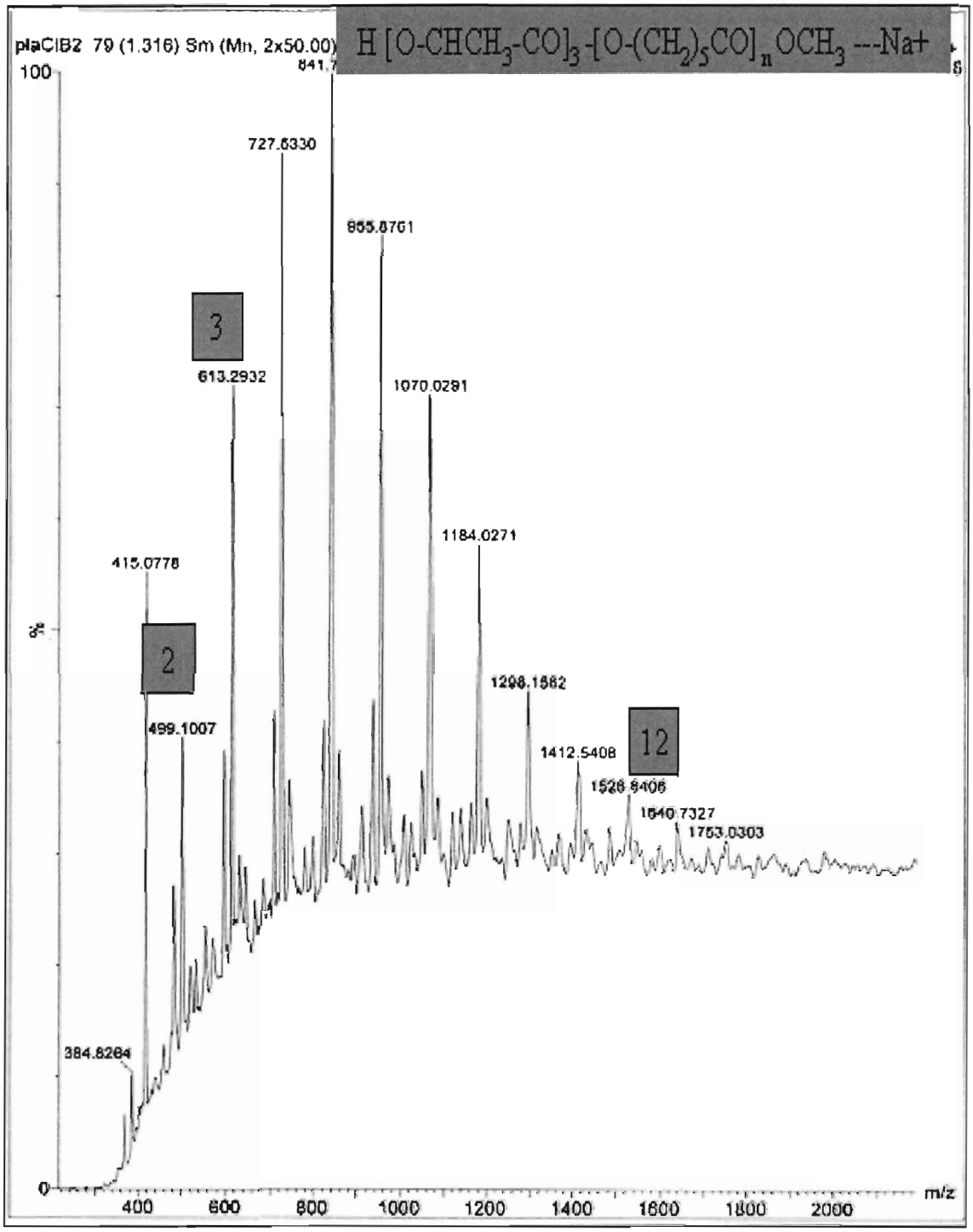

Figure 6.4 MALDI-TOF mass spectrum of Copolymer No.3 derived from PLLA and CL

Table 6.4 Structural assignments of the ions appearing in the expanded region at 450-550m/z of the MALDI-TOF mass spectrum of PLLA and P(LA-co-CL) copolymers listed in Table 6.2

No.	Peak in one unit	Mass formula
PLA	475 488	$H(LA)_6OH$ ---Na^+ $H(LA)_6OCH_3$---Na^+
2	499 517 540	$H(LA)_3$ Co $(CL)_2OCH_3$ ---Na^+ $H(LA)_3$ Co $(CL)_1OH$---Na^+ $H(LA)_2$ Co $(CL)_3OCH_3$ ---Na^+
4	481 499	$H(LA)_3$ Co $(CL)_2OH$---Na^+ $H(LA)_3$Co $(CL)_2OCH_3$ ---Na^+
5	481 499	$H(LA)_3$ Co $(CL)_2OH$---Na^+ $H(LA)_3$ Co $(CL)_2OCH_3$ ---Na^+

6.3.4 Differential scanning calorimetry

The thermal properties of the copolymers were investigated by differential scanning calorimetry (DSC). The DSC (first heating scan) curves of the copolymers are compared in Figure 6.5. The known glass transition temperature (T_g) value of the PLLA and polycaprolactone are 65°C and -60°C, respectively. The PLLA thermogram shows T_g value around 60°C and melting temperature(T_m) at 175°C. Copolymer No. 1 shows a broad T_m range with a peak at 150°C which may be due to a combination of CL and PLLA crystalline domains. In contrast, copolymer No. 2 show two distinct T_m ranges; the lower broader one with a peak at 50°C, corresponds to CL-rich crystalline domains while the higher narrower one with peak at 150°C corresponds to PLLA-rich domains. Since the Tm value of the copolymer no. 4 and 5 of 60°C are considerably closer to the Tg value of PCL (60°C) than PLL (171°C), it suggests that the amorphous phases are proportionately richer in CL than LA units. Finally, from their first heating scans, the copolymers are seen to be partially crystalline, indicating tapered rather than purely

random monomer sequencing.

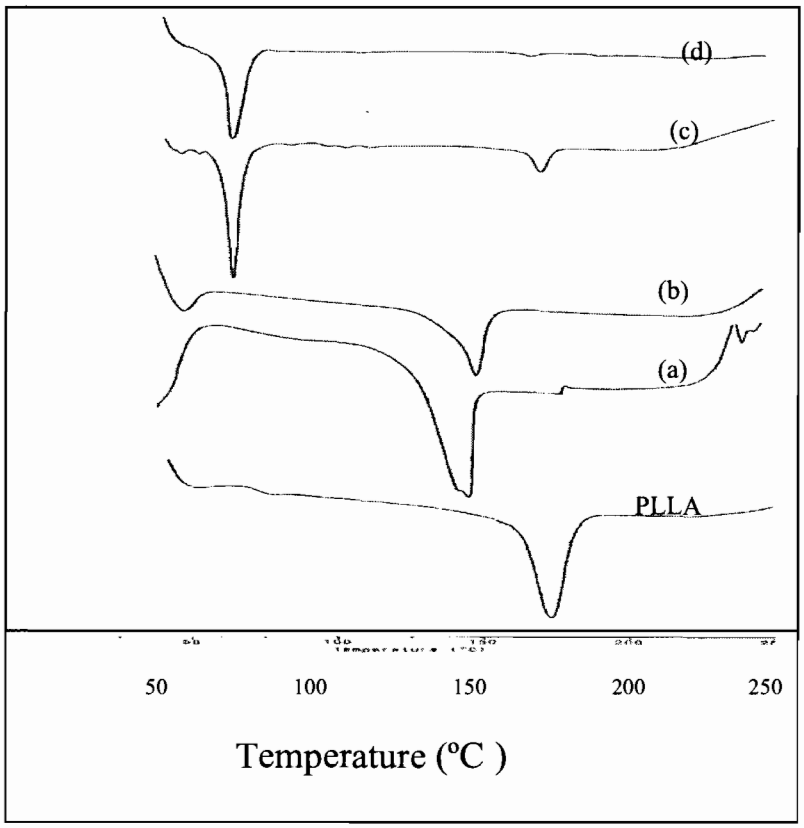

Figure 6.5 DSC thermograms (heating rate 10°C/min) from the first heating scans for the copolymer P(LA-co-CL) Nos: *(a)* 1;*(b)* 2; *(c)* 4 *(d)* 5 listed in Table 6.2

6.4 Conclusions

We have shown that new polymeric bio-materials, poly (L-lactic acid) can be modified by a one-step transesterification procedure to prepare P(LA-co-CL) copolymer with both controlled molecular weight and end functionality. By the amount of the ester compound added, here a ε–caprolactone, the molecular weight of the desired copolymer can be controlled. The formation of low molecular weight copolymer was confirmed by GPC and MALDI-TOF MS which revealed the addition of CL unit to PLLA. The structure of the copolymer was confirmed by 1H NMR. The well-resolved contributions

of chain end groups in the 1H NMR spectra can now be used to investigate the stages of the modification of PLLA polymers. The copolymer mainly consists of linear lactic acid unit and CL unit. It was found that a series of poly (lactic acid) could be transformed into the corresponding open ring copolymer P(LA-co-CL). By the copolymerization, P(LA-co-CL) was prepared for use as a compatibilizer for wood/PLLA composites. The CL groups of P(LA-co-CL) may react with the terminal OH groups of PLLA to create new linkages. DSC measurements revealed that the melting temperatures of modified PLLA decreased. Looking ahead to their possible applications in the field of bioplastic, CL monomer is considered to have potential to improve brittleness of PLLA due to their flexibility. Indeed, the effect of crosslinking on the mechanical properties of poly (lactic acid)/polycaprolactone blends has already been studied for the improvement of brittle behavior of poly (lactic acid) [41].

CHAPTER 7

Effects of P(LA-co-CL) on the Physical properties of wood-Poly (L-Lactic acid) Composites

7.1 Introduction

The property of wood fibers (WFs) with biodegradable polymers has been recently studied [42], and generally, the performance of these biomaterials is greatly influenced by both the properties of the fiber and the fiber/polymer-matrix adhesion. One of the most promising biodegradable polymers is poly (L-lactic acid) (PLLA), which can be derived from renewable resources, such as corn. Composites containing biodegradable polymers, such as PLLA, and WFs offer an interesting combination of properties as well as lower cost than competitive materials. PLLA is linear, aliphatic, thermoplastic polyester produced from an L-lactic acid byproduct obtained from the fermentation of corn dextrose. PLLA has many attractive features, such as good mechanical properties, but is still more expensive than the conventional plastics. WFs are attractive not only because of being cheap filler, but also of providing excellent properties to the final product. Therefore, WF/PLLA composite is meaningful because it reduces the total cost of the raw materials needed for the composite.

The main objective of this chapter is the study of the interfacial interactions of a compatibilizer for improving the performance of WF/PLLA composites, namely the mechanical properties. So, P(LA-co-CL), which have been reported in the previous chapter, was studied as a compatibilizer for WF/PLLA composites. The mechanical properties of the composites was determined and discussed.

7.2 Experimental method

7.2.1 Materials

The commercial grade of PLLA (Tensile strength=59MPa, elongation at break=2%, Modulus of elasticity=3040MPa, T_m=171 °C, T_g=57 °C), PL002, was supplied by

Kuraray, Japan. Wood fiber (WF), and bamboo fiber (BF) are used as the reinforcements in poly-L-lactic acid (PLLA). The composition of cellulose, hemicelluloses and lignin of two fibers are summarized in Table 7.1. The WFs (lignocel-C300G, Conifer Wood) were obtained from Rettenmaier and söhne, Germany and BF (*Phylioatachys pubescens*) was supplied by Nippon orimono kogyo, Japan. The compatibilizer used was P(LA-co-CL) copolymer prepared in laboratory and reported in the previous chapter.

Table 7.1 The composition of cellulose, hemicelluloses and lignin of two fibers

Fibers	Cellulose (%)	Hemicelluloses (%)	Lignin (%)
Wood	56.5	11.4	30.6
Bamboo	20.5	40.1	36.2

7.2.2 Processing

The fibers was compounded with PLLA and P(LA-co-CL) in a kitchen mixer at laboratory-scale. The wood fiber, PLLA, and compatibiliser No.3 P(LA-co-CL), were also sequentially mixed into a Super mixer, Kawata Mfg., Co., Ltd, Japan. The compounding process was conducted at a temperature of 180°C with a rotational speed of 1600rpm. After the compounding, the melts were removed from the mixer and cooled to room temperature. The formulations of the composite are given in Table 7.2. The compounds were then molded using a steel mold (Mold dimensions: $1\times8\times10cm^3$) by a Shinto hot press Model HCC-BSN-2. The hot-press platens were heated to 200°C before placing the compound filled mold on the bottom platen. The compounds were then hot-pressed for 15min under a pressure of 11MPa. The mold was then cooled at room temperature.

Table 7.2 The formulations of the composites prepared with different P(LA-co-CL) No.1, No.2, No.3, No.4 and No.5 listed in Table 6.2

No.	Composition	Weight ratio
1 [a]	BF/PLLA/No.3	80/20/0
2 [a]	BF/PLLA/No.3	80/20/0.02
3 [a]	BF/PLLA/No.3	80/20/0.2
4 [a]	BF/PLLA/No.3	80/20/1
5 [b]	WF/PLLA/No.3	80/20/0.2
6 [b]	WF/PLLA/No.3	80/20/0.4
7 [b]	WF/PLLA/No.3	80/20/0.6
8 [a]	WF/PLLA/No.1	80/20/0.2
9 [a]	WF/PLLA/No.2	80/20/0.2
10 [a]	WF/PLLA/No.4	80/20/0.2
11 [a]	WF/PLLA/No.5	80/20/0.2

[a] Compounds were mixed in Kitchen mixer; [b] Compounds were mixed in Super mixer;

7.2.3 Mechanical test

The mechanical properties (MOR and MOE) were measured in three-point bending tests using a standard material testing system (Shinto Model TCM-500l) at a crosshead speed of 5.0 mm/min in accordance with JIS A5908. The mechanical test specimens were also cut from the composite panels with dimensions of $0.25\times2.5\times10cm^3$.

7.2.4 Water absorption test

Water absorption and thickness swelling tests were conducted in accordance with JISA5908, in which the specimens were immersed in water for 24h at a room temperature. The weight gain and thickness swell were then measured 24h after being removed from the water. The calculation of the weight gain (Wt), and thickness swell (Th) of composites from the following equations:

$$Wt = (W_1 - W_0)/ W_0 \quad (1)$$

$$Th = (t_1 - t_0)/ t_0 \quad (2)$$

Where, W_1, W_0, t_1, and t_0 are the weight of the composite containing water, weight of the dried composite, thickness of wet composite and thickness of dry composite, respectively.

7.3 Results and discussion

7.3.1 Mechanical test

In order to improve the mechanical properties of the BF/PLLA and WF/PLLA composites, P (LA-co-CL) coupling agents were introduced for the increase of interfacial strength between the PLLA and fibers. The BF/PLLA and WF/PLLA composites containing 80% fiber and 20% PLLA were selected for investigating the effects of types and concentrations of P (LA-co-CL) coupling agents on the composite properties (Table 7.2). The chemical structures of four coupling agents used are also listed in Table 6.4. Figure.7.1 shows the modulus of rupture (MOR) and modulus of elasticity (MOE) of BF/PLLA composites added with 0.02%, 0.2% and 1% P(LA-co-CL) No. 3 coupling agent and Figure.7.2 presents the modulus of rupture (MOR) and modulus of elasticity (MOE) of WF/PLLA composites added with 0.2%, 0.4% and 0.6% P(LA-co-CL) No. 3 coupling agent. For both BF/PLLA and WF/PLLA composites, the MOR slightly increased to a maximum value around the P(LA-co-CL) No. 3 contents of 0.2wt%. After that, the MOR tended to decrease with 1% coupling agent content. Similar behavior was found for Modulus of elasticity (MOE) of the WF/PLLA composites. On the other hand, the decreases in the MOE of the BF/PLLA composites by the addition of coupling agent were attributed to two possible reasons which include an increase of interfacial defects or debonding between P (LA-co-CL) and BF phases. The optimum P(LA-co-CL) No. 3 concentration (around 0.2wt% of WF/PLLA) giving the maximum MOE in the composites clearly indicated high

interfacial interactions between the polymer molecule and wood fiber via the coupling agents. The MOR of the composites lies in the range of 13 and 18 MPa. The BF/PLLA composite exhibit higher MOR compared with the WF/PLLA composite. This is probably due to BF, which might enhance interface bonding.

Figure 7.3 shows the mechanical properties of WF/PLLA composites containing different coupling agent listed in Table 6.2. Generally, it was found that addition of coupling agent resulted increase in mechanical properties, which were referred to as MOR and MOE. The increase in MOR of the composites with No.1, No.2, No.3 and No.5 coupling agents were caused by compatibility between WF and PLLA phase. On the other hand, there is no change in MOR of the composite with No.4 coupling agent, indicating the incompatibility between strongly polarized WF and hydrophobic PLLA. It can be seen that the MOE slightly increased for all coupling agents. The effect was more pronounced for the composite with No.1 coupling agent.

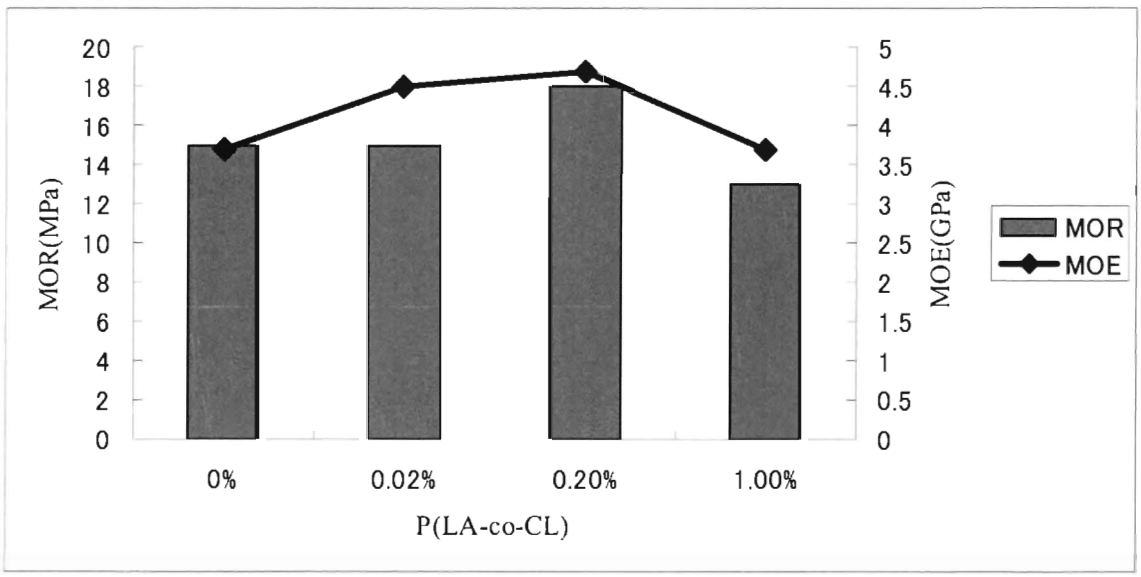

Figure 7.1 The MOR and MOE of BF/PLLA composites added with 0.02%, 0.2% and 1% of P(LA-co-CL) No. 3 listed in Table 6.2

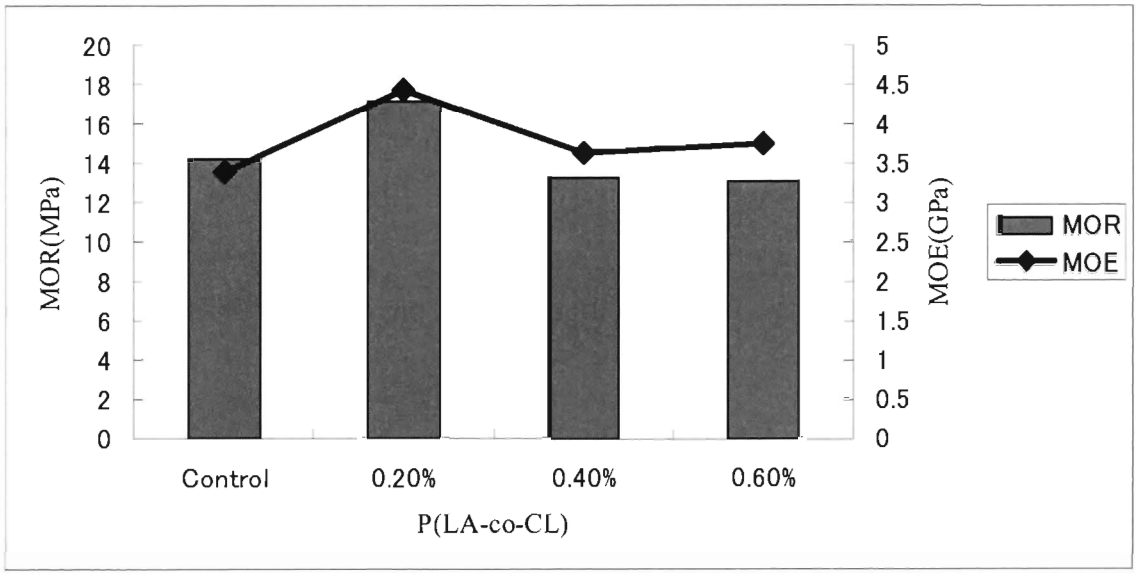

Figure 7.2 The MOR and MOE of WF/PLLA composites added with 0.2%, 0.4% and 0.6% of P(LA-co-CL) No. 3 listed in Table 6.2

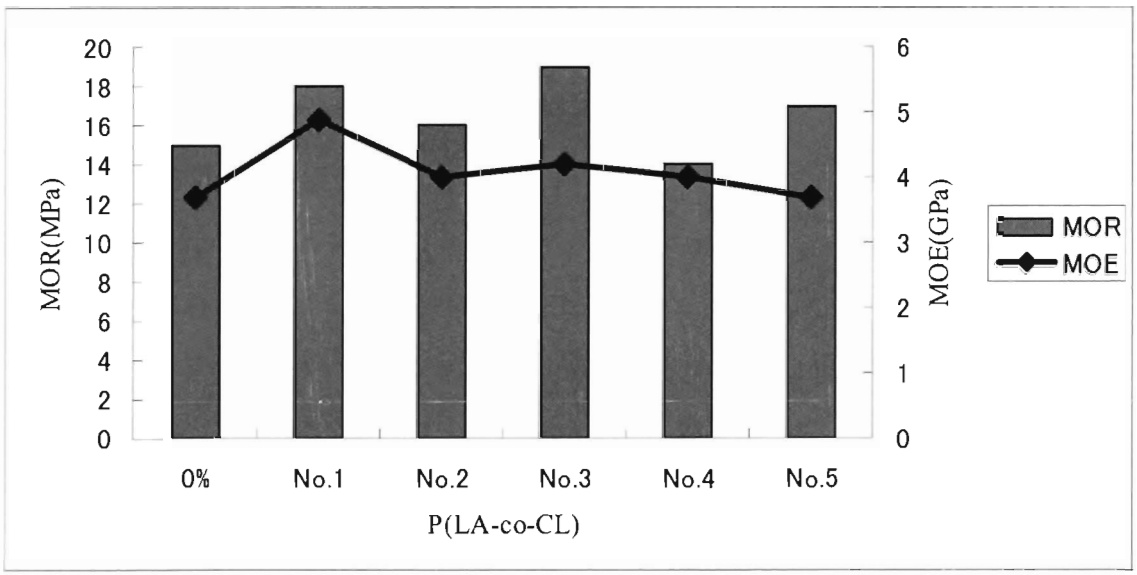

Figure 7.3 The MOR and MOE of WF/PLLA composites added with 0.2% of P(LA-co-CL) No. 1,2,3,4 and 5 listed in Table 6.2

7.3.2 Water absorption test

The weight gain values (Figure 7.4) for the BF/PLLA composites vary from 6% to 7.8%, and these values are decreased for WF/PLLA(Figure 7.5), varying from 5% to 6%. For BF/PLLA composites, the composite made with 0.02% and 0.2% content of coupling

agent have lower weight gain and lower thickness swell than composite without coupling agent. However, composites treated with 1% coupling agent show that thickness swell and weight gain are increased for BF/PLLA composites. In general, the WF/PLLA composite made with 0.2%, 0.4 and 0.6% coupling agent have increase in dimensional stability properties than without adding the coupling agent. On the other hand, the WF/PLLA composites made from higher coupling agent content have higher thickness swell and weight gain.

The weight gain (Figure 7.6) of the composites made with different coupling agent is from 4–6% after 24 h immersion in water. It is also noted that addition of coupling agent can not reduce the water absorption. The impact of wood to plastics ratio on the water absorption can be explained by the differences in water absorption between wood and plastics. The presence of hydroxyl and other polar groups in various constituents of the wood flour resulted in poor compatibility between the hydrophilic wood flour and the hydrophobic plastics, which increases the water absorption. Water absorption by cellulose and hemicelluloses depends on the number of free hydroxyl groups thus the amorphous regions are accessible by water.

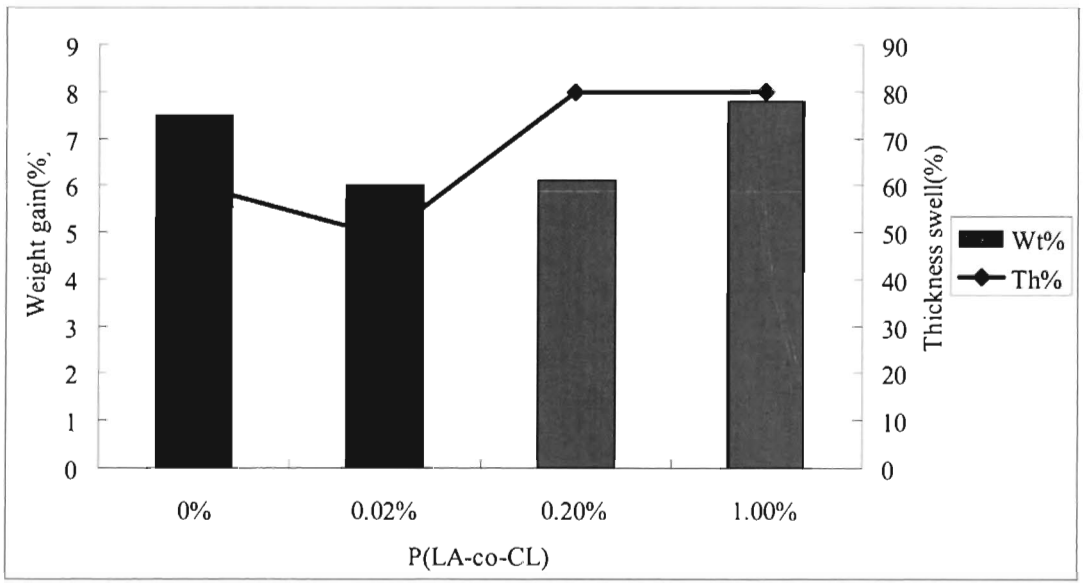

Figure 7.4 The weight gain and thickness swell after immersing 24hr of BF/PLLA composites added with 0.02%, 0.2% and 1% of P(LA-co-CL) No. 3 listed in Table 6.2

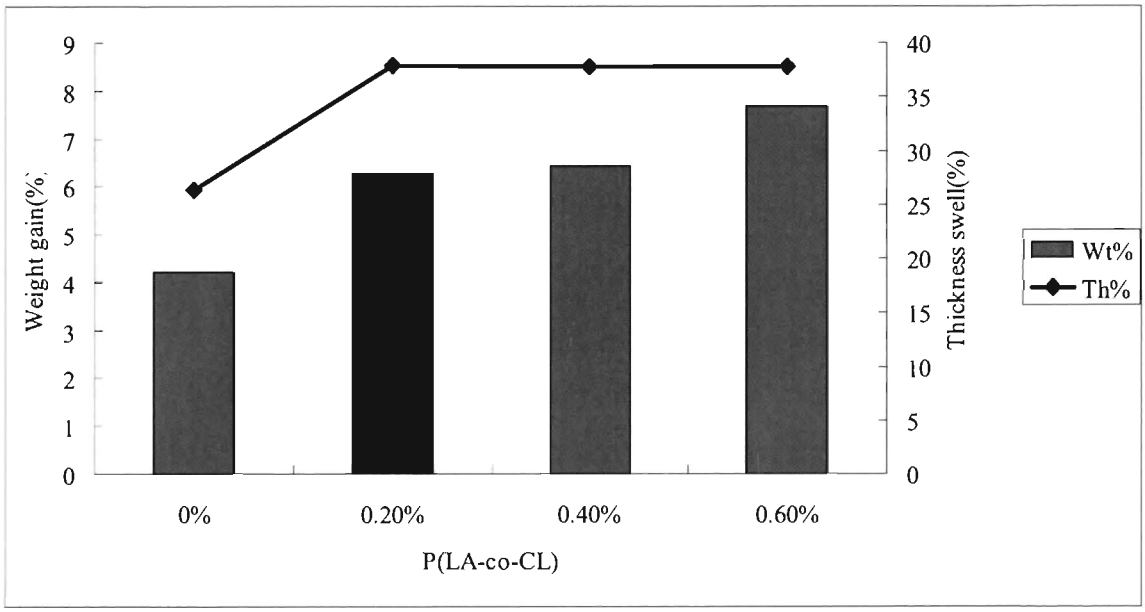

Figure 7.5 The weight gain and thickness swell after immersing 24hr of WF/PLLA composites added with 0.2%, 0.4% and 0.6% of P(LA-co-CL) No. 3 listed in Table 6.2

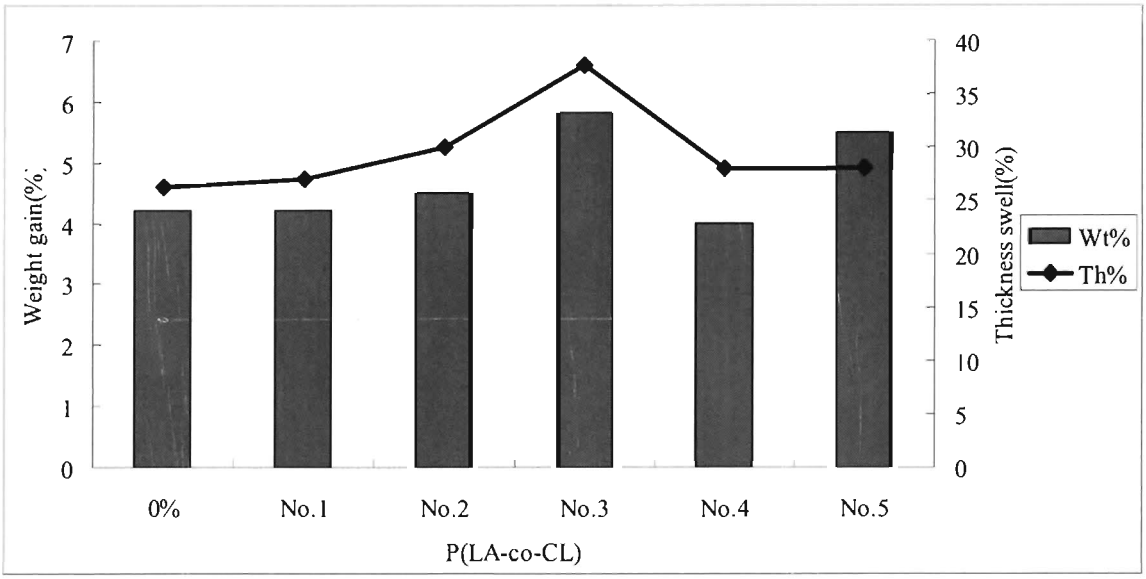

Figure 7.6 The weight gain and thickness swell after immersing 24hr of WF/PLLA composites added with P(LA-co-CL) no. 1,2,3,4 and 5 listed in Table 6.2

7.4 Conclusions

In this chapter, the mechanical and dimensional stability properties of BF/PLLA and WF/PLLA composites were studied by varying P(LA-co-CL) No.3 coupling agent contents, and different types of P(LA-co-CL) coupling agent. The results suggested that as the coupling agent content was increased, the modulus properties increased. Concentration of 0.2 wt% P(LA-co-CL) No.3 was recommended for the optimization of the mechanical properties of the composites, respectively. P(LA-co-CL) No.3 was more effective in terms of improving dimensional stability of the BF/PLLA composite

CHAPTER 8

Conclusion and Summary

8.1 Summary

The wood plastic composite (WPC) industry has progressed significantly over the past few years and WPC products are well established in North America, Europe and Japan. The ability for this market to grow will also depend upon the development of WPC containing high content of wood.

Two different highly filled WPCs were examined in this work. The first was based on cellulose micro fiber/polypropylene and Polypropylene modified with maleic anhydride (MAPP) with three different formulations and three different fiber lengths of cellulose. Cellulose/PP/MAPP composites were fabricated through four process engineering approaches: through compression molding by hydraulic press, compression molding by hot press, injection molding and extrusion molding. Since the engineering design of injection and extrusion molding of highly filled melts requires proper knowledge of the flow behavior, five formulations of cellulose/PP/MAPP, were produced by compounding in a conical twin-screw extruder, and the feasibility of compression, injection and extrusion molding was studied based on their flow behavior. The molded composites were characterized by thermal and mechanical properties, water absorption test, and observation of morphology.

The second WPC is with an 80/20 wood fiber/poly(L-lactic acid) (PLLA) composition containing modified PLLA as a compatibilizer. For modification of PLLA, a series of poly(lactic acid-co-ε-caprolactone)(P(LA-co-CL)) copolymers were synthesized by copolymerization of poly (L-lactic acid) and ε-caprolactone (CL) using hafnium chloride ($HfCl_4$) and $Sn(Oct)_2$ (tin(II) bis(2-ethylhexanoate)) as a catalyst. The resulting P(LA-co-CL) copolymers were characterized by various analytical techniques including matrix assisted laser desorption/ionization time-of-flight mass spectrometry (MALDI-TOF MS), gel permeation chromatography (GPC), and proton nuclear

magnetic resonance spectra (^{1}H NMR). The effect of coupling agent P(LA-co-CL) content on mechanical properties (MOR and MOE) and water resistance of composites was studied.

8.2 Effects of fiber length of cellulose on processibility and performance of cellulose/PP/MAPP composites

Processibility of compound with long fiber length is difficult than that of small fiber length. Because of loosely arranged fiber, composites of 900 μm long fiber and 90 wt% plastic content showed the highest swelling among the composites. The composite of small fiber showed good compatibility and good adhesion between the plastic and the cellulose fiber, while the composites of long fiber showed poor adhesion between the two phases. Composite density decreases when fiber length becomes increased.

8.3 Effects of fiber content on processibility and performance of cellulose/PP/MAPP composites

Strong composite with high percentage of filler greater than 70%, which is an order of higher percentage than that of conventional composites, has been developed. The melt flow index of the composite filled with 70 wt% of cellulose shows maximum packing. These features are unique for the cellulose fillers and provide a logical basis for achieving better processibility with cellulose at high filler loadings. These highly filled compounds may also be used in a low melt flow processing. As expected, the density of the composite decreases with increasing fiber content. The thermal stability of the materials showed that as the plastic content increases, coefficient of thermal expansion (CTE) increases as well. It is well known that the CTE of the polypropylene is greater than the cellulose polymer mixture, and thus, with increase of plastic content in the formulations the CTE of the resulting cellulose plastic increases. Thus, increasing the amount of plastic in the formulation gives a more flexible material. Storage modulus E' increased with an decrease in cellulose content for both injection molded composites and compression molding composites. Tan δ peak temperatures of composites

containing 70%cellulose were slightly shifted in comparison to that of PP, indicating improved adhesion and interaction between PP matrix and cellulose fibers.

8.4 Comparison of compression, injection and extrusion molding

In processing cellulose/PP/MAPP, it was shown that the feasibility of extrusion molding depended significantly on small fiber length but not as much the resin content. On other hand, injection molding was feasible with both low fiber content and smaller fiber length, and compression molded composites are feasible in all cases. It revealed that compression molding is more compatible. The mechanical properties of composites are influenced mainly by the adhesion between fiber and the matrix, and also tangle of fibers. It has been shown that the mechanical properties of cellulose/PP/MAPP composites depend significantly on the molding process. Compression molding composites molded by hot press exhibited the lowest modulus of rupture (MOR) and modulus of elasticity (MOE) and highest water absorption, while samples that were injection molded exhibited the highest MOR (70MPa) and MOE (7GPa) and low water absorption (2 wt%). The trend of water resistance of the composites is injection mold>extrusion mold>compression mold by hydraulic press>compression mold by hot press. We concluded that injection and extrusion molded composites, of cellulose/PP/MAPP, gave the best mechanical and physical properties. Extrusion molding allows better mixing of cellulose, thermoplastic polymer, and an additive because of the high shear of extrusion processing, which was elucidated by CCD micrographs. During thermal expansion analysis, the observed CTE values were significantly lower for the cellulose/PP/MAPP composites compared to the PP. The calculated CTE values of composites were in the range 2×10^{-5} to 4×10^{-5} which matched well with the range quoted in literature for WPC [4]. Every thermal transition implied a change in the decreasing slope of the $\log E'$ curve and the increase in the tan δ, which indicated that the blends became more viscous in nature with rising temperature. The storage modulus (E')-temperature relationship of most composites is characterized by

four transition points. The E' of compression molding composite AC filled with 80% cellulose exhibits highest value at 50°C.

8.5 Modification of poly (L-lactic acid)

Bio-based polyester such as, poly(L-lactic acid) can be modified by a one-step ring opening polymerization and so on to prepare copolymers with both controlled molecular weight and end functionality. In order to modify the PLLA γ-butyrolactone(BL), ε-Caprolactone(CL) and hydroxypivalic acid(HA) were used as impact modifier. It was found that the average molecular weights (MW) of P(LA-co-HA) and P(LA-co-CL) showed a slight change by the copolymerization. Regarding to the molecular weight distribution, bimodal distribution was observed in case of P(LA-co-BL) and P(LA-co-CL), but unimodal distribution was appeared in case of P(LA-co-HA). CL monomer is considered to have potential for modifying PLLA due to the low molecular weight of modifying products. Therefore, modification of PLLA by ε-caprolactone (CL) was examined in detail with a Lewis acid catalyst of hafnium (IV) chloride. The formation of low molecular weight copolymers was confirmed by MALDI-TOF MS which revealed the lactic acid repeating unit added opened ring caprolactone. Poly(L-lactic acid) can be modified by ε-caprolactone successfully.

8.6 P(LA-co-CL) copolymer as a compatibilizer

Copolymer P(LA-co-CL) can be referred as a compatibilizer. The compatibilizing mechanism of the P(LA-co-CL) used here, which has a relatively low molecular weight. It has been shown that the additive plays its role as a compatibilizer for both BF/PLLA and WF/PLLA composites. It improved adhesion between the filler (BF and WF) and matrix polymer PLLA. The P(LA-co-CL) also behaves as water resistant additive because it reduces the water absorption for BF/PLLA. The analysis of mechanical strength of composite showed that there is slight increase in MOR and MOE in the presence of a small amount of P(LA-co-CL), but beyond P(LA-co-CL) content of 0.2 wt %, the mechanical property of the composite decreases due to the lower

compatibility between P(LA-co-CL) and the PLLA matrix. This study suggests that there is a critical amount of P(LA-co-CL) at which it exhibits the strong interactions with wood fibers as well as the P(LA-co-CL) matrix.

8.7 Comparision of cellulose/PP/MAPP and wood/PLLA composites

The mechanical properties of wood/PLLA are weaker than the cellulose/PP/MAPP, indicating that the deforming capacity of cellulose facilitates the denser packing of the filler particles. The cellulose/PP/MAPP composites gave better results in comparison with wood/PLLA composite.

ACKNOWLEDGMENTS

First of all I would like to thank Dr. Okamoto Tadashi, my advisor and mentor, for all the help, support, and advice that he has provided me through this journey known as graduate school. I appreciate his vast knowledge and skill in many areas (e.g., organic chemistry, wood-plastic composites, adhesives, green chemistry, interaction with students), and his assistance in writing reports (scholarship applications, paper, and this thesis)

Very special thanks to Dr. Masahiro Takatani, is the one professor of our laboratory, without whose motivation and encouragement I would not have considered a graduate career in this research. I must also acknowledge Mr. Hirokazu Ito of the Yamaha Living Tech for his suggestions for, and provision of the materials evaluated in this study. I would like to thank all the members of the Taiyo Gosei family. They are invaluable for helping in extrusion molding process. I wish to express my warm and sincere thanks to Dr. Takashi Kitayama.

I would like especially like to thank Mr. Ikeda whose technical support made this research possible. I would also like to express my appreciation to Miss Miho Uchiyama and Mr. Koga for helping me with the laborious task of experiments. I would also like to thank my friends in the Laboratory of Biomaterials.

I would also like to thank my family for the support they provided me through my entire life and in particular, I must acknowledge my husband, Dr. Arun, without whose encouragement and editing assistance, I would not have finished my PhD. Most of all I want to thank my parents for their love and support.

In conclusion, I recognize that this research would not have been possible without the financial assistance of Gakujutsu Frontier Research Assistance ship, the Nara Ken Scholarship, the Kinki University Graduate School Scholarships and Japan Student Services Organization (JASSO) Graduate School Scholarship, and express my gratitude to those agencies.

REFRENCES

1. A. K. Mohanty, M. Misra, and G. Hinrichsen (2000) Biofibres, biodegradable polymers and biocomposites: An overview. Macromol. Mater. Eng. 276/277:1–24
2. Anatole A. Klyosov (2007) Wood-Plastic Composites, Wiley, USA, Chapter 1
3. Stark NM, Matuana LM (2004) Surface chemistry and mechanical property changes of wood-flour/high-density-polyethylene composites after accelerated weathering. J Appl Polym Sci 94:2263–2273
4. Li TQ, Wolcott MP (2005) Rheology of wood plastics melt. Part 1. Capillary rheometry of HDPE filled with maple. Polym Eng Sci45:549–559
5. Li TQ, Ng CN, Li RKY (2001) Impact behavior of sawdust/recycled–PP composites. J Appl Polym Sci 81:1420–1428
6. Patil YP, Gajre B, Dusane D, Chavan S, Mishra S (2000) Effect of maleic anhydride treatment on steam and water absorption of wood polymer composites prepared from wheat straw, cane bagasse, and teak wood sawdust using Novolac as matrix. J Appl Polym Sci 77:2963–2967
7. La Mantia FP, Morreale M, Mohd Ishak ZA (2005) Processing and mechanical properties of organic filler-polypropylene composites. J Appl Polym Sci 96:1906–1913
8. Li TQ, Wolcott MP (2004) Rheology of HDPE–wood composites.I. Steady state shear and extensional fl ow. Compos Part A ApplSci Manufact 35:303–311
9. Li TQ, Wolcott MP (2006) Rheology of wood plastics melt, part 2: effects of lubricating systems in HDPE/maple composites. Polymer Eng Sci 46:464–473
10. David N.-S. Hon, Nobuo Shiraishi (2001) Wood and Cellulosic Chemistry, Second Edition, Marcel Dekker, Inc., USA, Chapter 2
11. Eero Sjostrom (1993) Wood Chemistry: Fundamentals and Applications, Second Edition, Academic Press, USA, Chapter 1
12. Dinesh Mohan, Charles U. Pittman, and Philip (2006) Pyrolysis of Wood/Biomass

for Bio-oil: A Critical Review, Energy Fuels, 20 (3): 848 -889

13. Karin Hofstetter1, Barbara Hinterstoisser and Lennart Salme (2006) Moisture uptake in native cellulose – the roles of different hydrogen bonds: a dynamic FT-IR study using Deuterium exchange, Cellulose Springer 13:131–145
14. Roger M. Rowell, Roger Pettersen, James S. Han, Jeffrey S. Rowell, and Mandla A. Tshabalala (2005) Cell Wall Chemistry, Handbook of Wood Chemistry and Wood Composites, CRC Press, USA, Chapter 3
15. Badal C. Saha (2003) Hemicellulose bioconversion, Journal of Industrial Microbiology and Biotechnology 30: 279–291
16. Hans Önnerud, Liming Zhang, Göran Gellerstedt, and Gunnar Henriksson (2002) Polymerization of Monolignols by Redox Shuttle–Mediated Enzymatic Oxidation: A New Model in Lignin Biosynthesis I, Plant Cell 14(8): 1953–1962
17. W. Heinen, S. W. Erkens, M. Van Duin, J. Lugtenburg (1999) Model Compounds and 13C NMR Increments for the Characterization of Maleic Anhydride-Grafted Polyolefins, Journal of Polymer Science: Part A: Polymer Chemistry, 37: 4368–4385
18. W. Heinen, C. H. Rosenmoller, C. B. Wenzel, H. J. M. de Groot and J. Lugtenburg, M. van Duin (1996) 13C NMR Study of the Grafting of Maleic Anhydride onto Polyethene, Polypropene, and Ethene-Propene Copolymers, Macromolecules, 29: 1151-1157
19. M. Avella, L. Casale, R. Dellerba, B. Focher, E. Martuscelli, A. Marzetti (1998) Broom Fibers as Reinforcing Materials for Polypropylene-Based Composites, J Appl Polym Sci 68: 1077–1089
20. Chin-San Wu (2004) Analysis of Mechanical, Thermal, and Morphological Behavior of Polycaprolactone/Wood Flour Blends, Journal of Applied Polymer Science, 94: 1000–1006
21. Seung-Hwan Lee, Tsutomu Ohkita and Kazuo Kitagawa (2004) Eco-composite from poly(lactic acid) and bamboo fiber, Holzforschung, 58: 529–536
22. Roger M. Rowell, R. Asaletha, G. Groeninckk, M. G. Kumaran, Sabu Thomas

(1998) Advances and Challenges of Wood Polymer Composites, Proceedings of the 8th Pacific Rim Bio-Based Composites Symposium

23. Melt Rheology and Morphology of Physically Compatibilized Natural Rubber–Polystyrene Blends by the Addition of Natural Rubber-g-Polystyrene, Journal of Applied Polymer Science 69: 2673–2690
24. Caraschi JC, Leão AL (2002) Wood flour as reinforcement of polypropylene. Mater Res 5: 405–409
25. Brandrup J, Immergut EH, Grulke EA, Abe A, Bloch DR (1999) Polymer handbook, 4th edn. Wiley, New York, p II/475
26. L. Chotirat, K. Chaochanchaikul, N. Sombatsompop (2007) On adhesion mechanisms and interfacial strength in acrylonitrile–butadiene–styrene/wood sawdust composites International Journal of Adhesion & Adhesives 27: 669–678
27. Magnus Bengtsson a, Paul Gatenholm b, Kristiina Oksman (2005) The effect of crosslinking on the properties of polyethylene/wood flour composites. Composites Science and Technology 65 : 1468–1479
28. Magnus Bengtsson , Kristiina Oksman (2006)Silane crosslinked wood plastic composites: Processing and properties Composites Science and Technology 66: 2177-2186
29. Geimer RL, Clemons CM, Wood, JE (1993) Density range of compression-molded polypropylene-wood composites. Wood Fiber Sci 25(2): 163-169
30. Qiu W, Zhang F, Endo T, Hirotsu T (2004) Milling-induced esterification between cellulose and maleated polypropylene. J Appl Polym Sci 91:1703–1709
31. Qiu W, Endo T, Hirotsu T (2004) Interfacial interactions of a novel mechanochemical composite of cellulose with maleated polypropylene, J Appl Polym Sci 94: 1326–1335
32. R. Gosselin, D. Rodrigue, and B. Riedl (2006) Injection Molding of Post consumer Wood–Plastic Composites II: Mechanical Properties, Journal of Thermoplastic Composite Materials 19: 659
33. Bussu G., Lazzeri A. (2006) On the use of dynamic mechanical thermal analysis

(DMTA) for measuring glass transition temperature of polymer matrix fibre reinforced composites Journal of Materials Science 41: 6072-6076

34. Sun-M. Lai , Feng-C. Yeh , Yeh Wang , Hsun-C. Chan , Hsiao-F. Shen (2003) Comparative study of maleated polyolefins as compatibilizers for polyethylene/wood flour composites, J Appl Polym Sci 87: 487-496
35. Sanjeev Singh and A.K. Mohanty (2007) Wood fiber reinforced bacterial bioplastic composites: Fabrication and performance evaluation Composites Science and Technology 67: 1753-1763
36. Jacob John, Jian Tang, Zhihong Yang, Mrinal Bhattacharya (1997) Synthesis and characterization of anhydride-functional polycaprolactone, Journal of Polymer Science Part A: Polymer Chemistry, 35: 1139-1148
37. Denise Carlson, Li Nie, Ramani Narayan, Philippe Dubois (1999) Maleation of polylactide (PLA) by reactive extrusion, Journal of Applied Polymer Science 72: 477-485
38. Kaiyong Cai, Kangde Yao, Songbai Lin, Zhiming Yang, Xiuqiong Li, Huiqi Xie, Tingwu Qing and Laibao Gao (2002) Poly(D,L-lactic acid) surfaces modified by silk fibroin: effects on the culture of osteoblast in vitro, Biomaterials 23:1153-1160
39. Naotsugu Nagasawa, Ayako Kaneda, Shinichi Kanazawa, Toshiaki Yagi, Hiroshi Mitomo, Fumio Yoshii and Masao Tamada (2005) Application of poly(lactic acid) modified by radiation crosslinking, Nuclear Instruments and Methods in Physics Research Section B: Beam Interactions with Materials and Atoms 236: 611-616
40. Gea Raldine Coullerez, Christian Lowe, Peter Pechy, Hans Henning Kausch, Joe Ns Hilborn (2000) Synthesis of acrylate functional telechelic poly(lactic acid) oligomer by transesterification, Journal Of Materials Science: Materials In Medicine 11: 505
41. Takeshi Semba, Kazuo Kitagawa, Umaru Semo Ishiaku, Hiroyuki Hamada (2006) The Effect of Crosslinking on the Mechanical Properties of Polylactic Acid/Polycaprolactone Blends, Journal of Applied Polymer Science 101: 1816–1825

42. M. S. Huda, L. T. Drzal, M. Misra, A. K. Mohanty (2006) Wood-Fiber Reinforced Poly(lactic acid) Composites: Evaluation of the Physicomechanical and Morphological Properties, Journal of Applied Polymer Science 102: 4856–4869
43. Xiaolin Cai, Bernard Riedl, S. Y. Zhang, Hui Wan (2007) Effects of Nanofillers on Water Resistance and Dimensional Stability of Solid Wood Modified by Melamine-Urea-Formaldehyde Resin , Wood and Fiber Science 32: 307-318
44. Huang J, Zhang L, Wang X (2003) Soy protein–lignosulphonate plastics strengthened with cellulose. J Appl Polym Sci 89:1685–1689
45. Atsuhiko Yamanaka, Yoshinobu Izumi, Tooru Kitagawa, Takaya Terada, Hiroshi Hirahata, Kimiko Ema, Hiroyuki Fujishiro, Shigehiro Nishijima (2006) The effect of γ-irradiation on thermal strain of high strength polyethylene fiber at low temperature. J Appl Polym Sci 102:204–209